Exploring the Interface Between Plasmas and Liquids

Addressing Contemporary Challenges with Innovative Software Tools

Davide Curreli

dcurreli@illinois.edu

Nuclear, Plasma, and Radiological Engineering
University of Illinois at Urbana Champaign

LCPP Laboratory of Computational Plasma Physics – Software

Plasma Fluid Models

1. **CRANE** (Plasma Chemistry)
   https://github.com/lcpp-org/crane
2. **ZAPDOS** (Plasma Transport)
   https://github.com/shannon-lab/zapdos

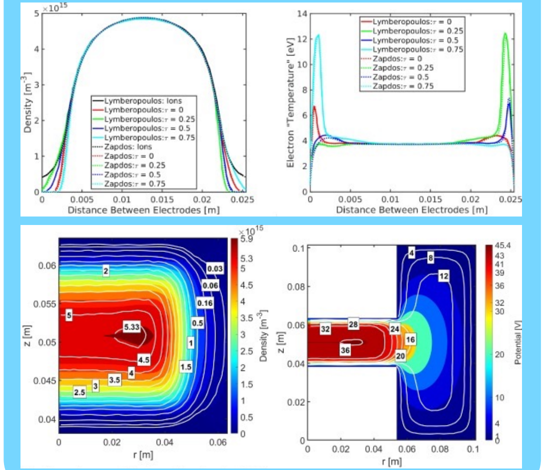

Ion-Surface Interactions

1. **RustBCA**

   https://github.com/lcpp-org/RustBCA

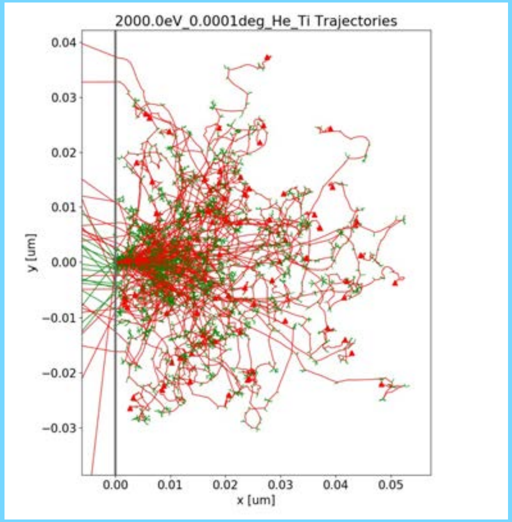

Plasma Kinetic Models

1. **hPIC** (MPI/OpenMP)
   https://doi.org/10.1016/j.cpc.2018.03.028
2. **hPIC2** (+GPU)
   https://doi.org/10.1016/j.cpc.2022.108569

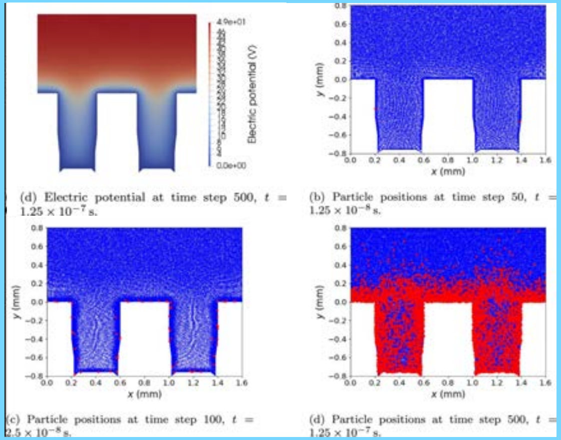

Main Question: How do we model a plasma interacting with liquid water?

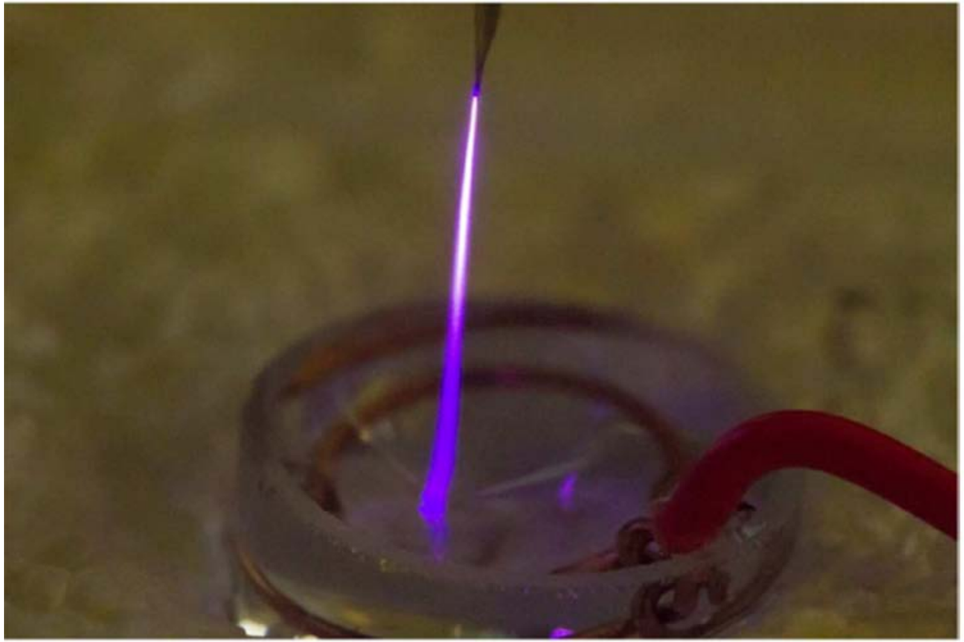

[Fig adapted from: Lindsay, A. et al. J. Phys. D: Appl. Phys. 48 (2015) 424007]

Outline

1. **Motivation & Background**
   1. Why plasma-water interactions are relevant?
   2. Societal benefits
2. **A New Open-Source MOOSE-Based Application for Low-Temperature Plasmas**
   1. CRANE: chemical kinetics software
   2. ZAPDOS: plasma transport software
   3. Verifications of Zapdos-Crane
3. **Case Study: Plasma Electrochemical Cell**
   1. Ar/H_2O humid argon plasma interacting with liquid water
   2. Species in the gas and liquid phases
   3. Aqueous Charge Balancing
   4. Reactive Species Generation
   5. Solvated Electrons at the Interface
4. **Conclusions**

Motivation: Plasma-Water Interactions

Applications

- **Generation of reactive oxygen and nitrogen species**
  - Antimicrobial properties
  - Ammonia production
  - Wound disinfection and healing
  - And more
- **Other, domain specific**
  - Plasma medicine
  - Synthesize graphene particles and nanosheets
  - Toxic metal detection
  - And much more

Advantages

- **Cheap and abundant materials**
- **“Cold” plasma - useful for thermally sensitive surfaces**
  - heat-sensitive equipment
  - bodily wounds

NO2- production in a plasma-water reactor.

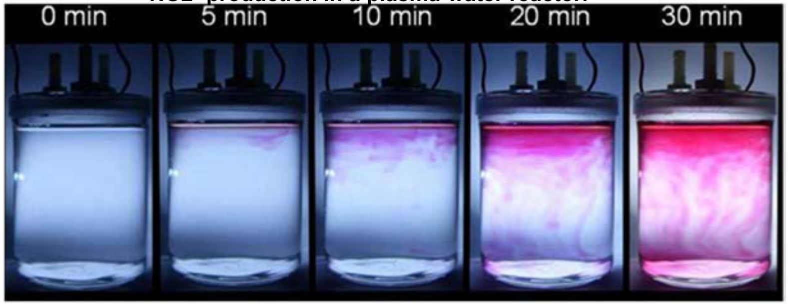

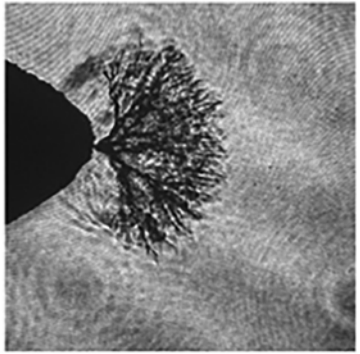

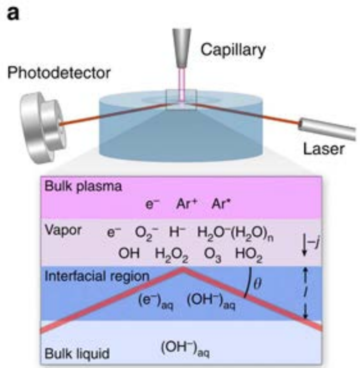

Top: NO2- production in a plasma-water reactor. [1]
Bottom-right: Schematic of solvated electron measurement experiment. [2]
Bottom-left: Streamers propagating in liquid water. [3]

[1] Oehmigen K. IEEE Trans. Plasma Sci. 39 2646 (2011)
[2] Rumbach, P. *et al.* Nature Communications 6 7248 (2015)
[3] Foster, J., Physics of Plasmas 24 055501 (2017)

Methods

- **Plasma-in-liquid**
  - Directly ionize water phase with high voltages
  - Requires high voltages, but good source of OH production
- **Bubble plasmas**
  - Gas composition of bubbles may be tailored to adjust chemistry
- **Plasma-liquid interface**
  - Plasma generated in gas phase
  - Transport of reactive species depends on diffusion through water interface
  - Electrons drive RONS production by entering water phase and solvating

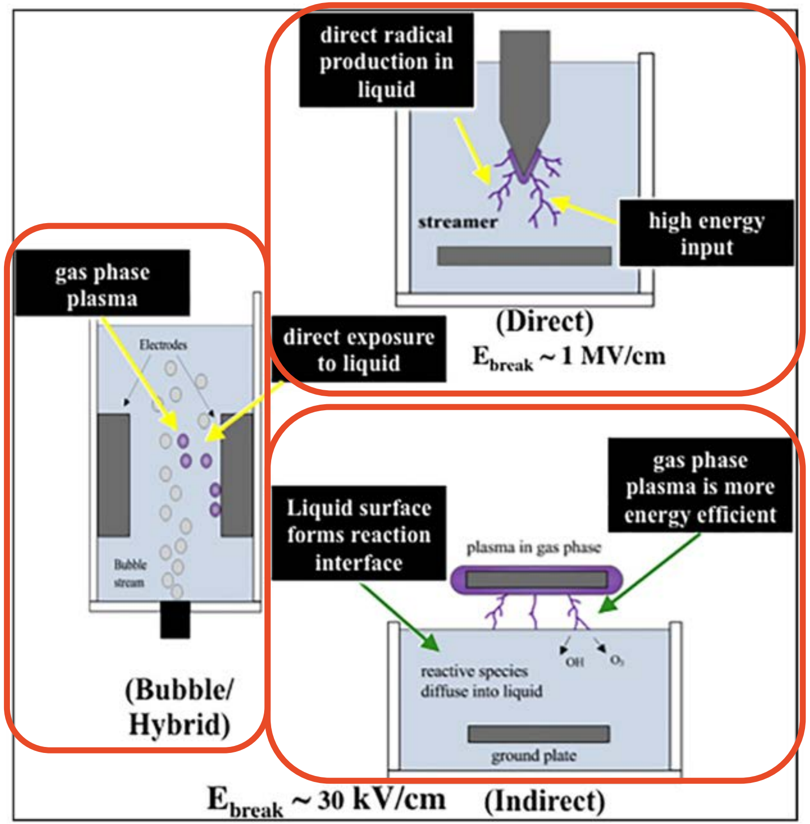

Figure adapted from [3].

[3] Foster, J. *Plasma-based water purification: Challenges and prospects for the future.* Physics of Plasmas 24 055501 (2017)

Plasma-liquid interfaces: a challenge for modern plasma modeling

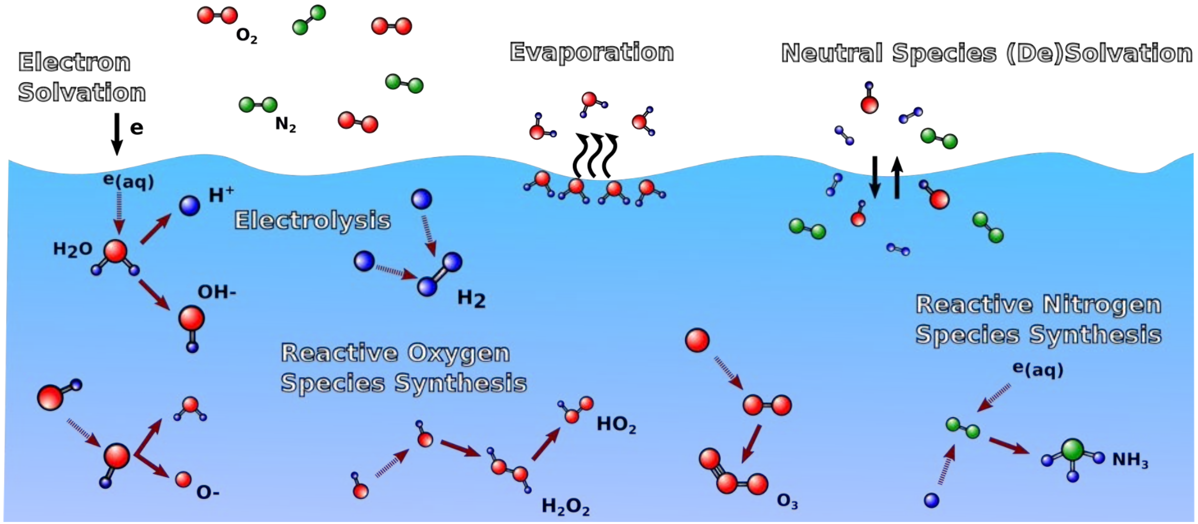

- **Multiscale and multiphysics**
  - Electron penetration depth: ~10-100 nm
  - Discharges: mm-cm
  - Electron solvation: O(fs)
  - Electron-driven aqueous reactions: O(ns)
  - Chemical reactions: O(us-ms)
  - Species diffusion: O(ms - minutes)
- **Strongly coupled behavior between plasma and water**
  - Electrons drive chemistry in the interface layer, which change chemical composition of the water
  - Species diffuse in and evaporate out of interface, modifying plasma discharge conditions
  - Electric fields, gas flow can deform water
  - Plasma-induced fluid convection and turbulence is possible

Plasma Chemistry modeling requires information at multiple levels

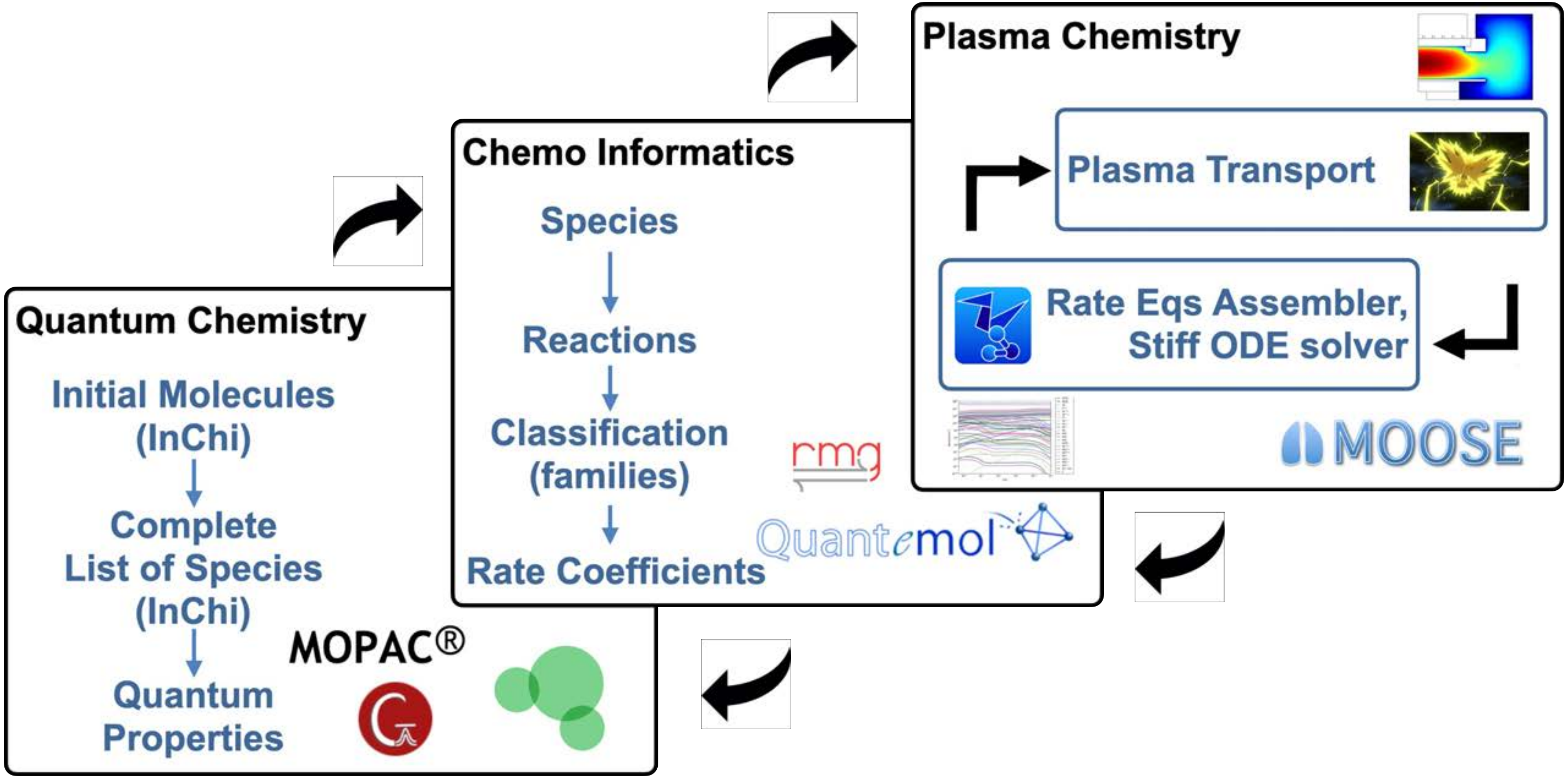

New software tools: Zapdos and Crane

- **Plasma-liquid interfaces are notoriously nonlinear, multiscale in both space and time, and multiphysics**

- **The MOOSE finite element framework was selected as an appropriate platform for development of a general plasma software package**
  - MOOSE applications are natively parallelizable and intended for high performance computing (HPC)
  - All MOOSE apps are able to be coupled together, facilitating multiphysics simulations

- **The MOOSE app Zapdos[4] was developed specifically for modeling plasma transport in 2015-2016**
  - As of 2017, only included support for electron and argon discharges

- **No chemistry capabilities were included in the MOOSE framework, and Zapdos was hard-coded to accept only a handful of reactions**

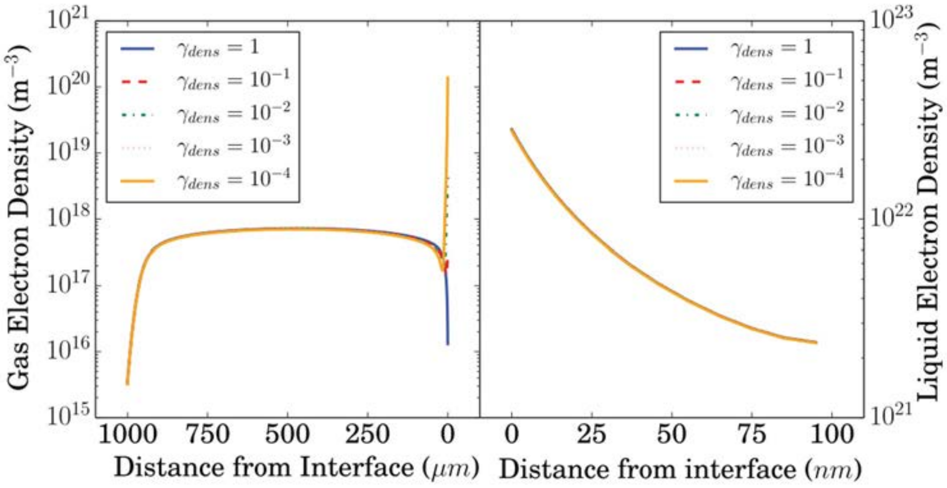

Electron density as a function of interfacial loss coefficient in the gas phase (left) and water phase (right). Simulation was performed with Zapdos. Figure adapted from [4].

[4] Lindsay, A. *et al.* J. Phys. D: Appl. Phys. *49* (2016) 235204 (9pp)

[5] C. DeChant, S. Keniley, D. Curreli, K. Stapelmann, S. Shannon, "Multi-physics simulation of the COST APPJ in the MOOSE framework", Bull. Am. Phys. Soc. 71th Annual Gaseous Electronic Conference, GT1.74, Portland, Oregon, Nov 5-9, 2018

Model Development at LCPP

- As of 2017, Zapdos was hard-coded to accept only four species (e^-, Ar^+ in the gas phase, and $e^-_{(aq)}$ and $OH^-_{(aq)}$ in the water), with 5 total reactions.
- As part of NSF-funded research, we introduced two new capabilities:

1. Developed Plasma Chemistry Application in MOOSE: "CRANE"

https://github.com/lcpp-org/crane

- Written a model capable of handling an arbitrary number of reactions
- Reactions can be automatically parsed by code into source and sink terms
- Coupled to Zapdos to add source terms to drift-diffusion equations

2. Upgraded Zapdos

https://github.com/shannon-lab/zapdos

- Allowed an arbitrary number of user-defined species
- Included surface charge accumulation
- Upgraded water model to include neutral transport across interface

ZAPDOS: Drift-Diffusion-Reaction Equations

Volumetric Terms:

Species Density:

$$\frac{\partial n_s}{\partial t} + \nabla \cdot \vec{\Gamma}_s = \boxed{R_{sr}}$$

Electron Energy:

$$\frac{\partial (n_e \epsilon)}{\partial t} + \nabla \cdot \vec{\Gamma}_\epsilon = \underbrace{-e\vec{\Gamma}_e \cdot \vec{E}}_{\textit{Joule Heating}} + \boxed{R_{sj,\epsilon}}$$

$$\vec{\Gamma}_s = \pm \mu_s \vec{E} n_s - D_s \nabla n_s$$

$$\vec{\Gamma}_\epsilon = -\tfrac{5}{3}\epsilon \vec{\Gamma}_e - \tfrac{5}{3} n_e D_e \nabla \epsilon$$

Poisson Equation:

$$-\nabla^2 \phi = \frac{\left(\sum_i q_i n_i + q_e n_e\right)}{\epsilon_0}$$

Boundary Conditions [6]:

Electron BC:

$$\vec{\Gamma}_e \cdot \hat{n} = \frac{1 - r_e}{1 + r_e} \left[-(2a - 1)\mu_e \vec{E} \cdot \hat{n} n_e + \tfrac{1}{2} v_{th_e} (n_e - n_\gamma)\right] - \tfrac{2}{1+r_e}(1-a)\textstyle\sum_p \gamma_p \vec{\Gamma}_p \cdot \hat{n}$$

Ion/Netural BC:

$$\vec{\Gamma}_h \cdot \hat{n} = \frac{1 - r_h}{1 + r_h}\left[(2a - 1) \pm \mu \vec{E} \cdot \hat{n} n_h + \frac{1}{2} v_{th} n_h\right]$$

Reaction Rates:

$$R_{sj} = \textstyle\sum_j \nu_{sj} k_j \prod_r^R n_r$$

$$R_{sj,\epsilon} = \textstyle\sum_j \nu_{sj} k_j \prod_r^R n_r \Delta\epsilon_j$$

[6] Hagelaar, G. *et al*. Physical Review E. *62*, 1 (2000)

1. CRANE: Chemical Kinetics

- **Crane is a standalone Moose application developed as part of the previous NSF work focused on modeling arbitrary systems of ODEs**
- **Source code:** https://github.com/lcpp-org/crane
- **When coupled to Zapdos, it provides the reaction rate portion of the drift-diffusion-reaction system**

$$\frac{dn_s}{dt} = \sum_{r=1}^{r_{max}} K_{sr}$$

$$K_{sr} = \nu_{sr} k_r \prod_l n_l^L$$

Stoichiometric Coefficient — *Rate Coefficient* — *Product of all Reactants for reaction r*

- **Electron-impact reactions preprocessed with external Boltzmann solver (Bolsig+, LoKI)**
  - Integral of EEDF $k_r = \gamma \int_0^\infty \varepsilon \sigma_r f_0 d\varepsilon$
  - Calculates rate coefficients (k) and electron transport coefficients
  - Values stored in look-up tables for a range of mean electron energies

- **Developed to allow an arbitrary number of reactions to be added in a human-readable format**

Reaction	Rate Coefficient	Units
$e + Ar \rightarrow e + Ar$	EEDF	$m^3\ mol^{-1}\ s^{-1}$
$e + Ar \rightarrow Ars + e$	EEDF	
$e + Ars \rightarrow e + Ar$	EEDF	
$e + Ar \rightarrow 2e + Ar^+$	EEDF	
$e + Ars \rightarrow 2e + Ar^+$	EEDF	
$Ars + Ars \rightarrow e + Ar + Ar^+$	3.3734×10^8	
$Ars + Ar \rightarrow Ar + Ar$	1.807×10^3	

Typical reaction list you find in a paper

How you write it in CRANE:

```
[Reactions]
  [argon_reactions]
    species = 'em Ar+ Ar*'
    file_location = 'rate_files'
    potential = 'potential'


    reactions = 'em + Ar -> em + Ar                     : EEDF [elastic] (reaction1)
                 em + Ar -> em + Ar*                    : EEDF [-11.5]   (reaction2)
                 em + Ar* -> em + Ar                    : EEDF [11.5]    (reaction4)
                 em + Ar -> em + em + Arp               : EEDF [-15.76]  (reaction3)
                 em + Ar* -> em + em + Arp              : EEDF [-4.43]   (reaction5)
                 Ar* + Ar* -> em + Ar + Arp             : 3.3734e8'
                 Ar* + Ar -> Ar + Ar                    : 1807
  []
[]
```

[7] S. Keniley, D. Curreli, C. DeChant, S. Shannon, CRANE: a Novel MOOSE-based Open-Source tool for Plasma Chemistry Applications and Code Coupling, Bull. Am. Phys. Soc., GT1.39, Portland, Oregon, Nov 5-9, 2018

2. Upgrades to Zapdos

Source code: https://github.com/shannon-lab/zapdos

Zapdos required multiple updates to address realistic plasma-water chemistry:

2.1 Accept arbitrary number *s* of user-defined plasma species

2.2 Add surface charge accumulation for dielectric interfaces

2.3 Include heavy species solvation and evaporation boundary conditions

$$\frac{\partial n_s}{\partial t} + \nabla \cdot \vec{\Gamma}_s = R_{sr}$$

$$\vec{\Gamma}_s = \pm \mu_s \vec{E} n_s - D_s \nabla n_s$$

$$-\nabla^2 \phi = \frac{\left(\sum_i q_i n_i + q_e n_e\right)}{\epsilon_0}$$

2. Upgrades of Zapdos

2.1 Accept arbitrary number of user-defined species

- Existing code was abstracted to include arbitrary species variables
- A new class, ‘**HeavySpeciesMaterial’,** was added to add species properties (mass, charge, transport coefficients)
- Mobility and diffusivity are by default given by Einstein’s relation (user can change)

```
[gas_species_example]
  type = HeavySpeciesMaterial
  heavy_species_name = Ar+
  heavy_species_mass = 6.64e-26
  heavy_species_charge = 1.0
  diffusivity = 1.6897e-5
[]
```

$$\mu_s = \frac{Z_s q_e D_s}{k_B T_e}$$

2. Upgrades of Zapdos

2.2 Added surface charge accumulation for dielectric interfaces

- Dielectrics are widely used in plasma discharges, but no interface existed in Zapdos to handle surface charge accumulation

- Surface charge was added to the model in two parts:
  a. ODE at dielectric boundary to describe surface charge accumulation
  b. Interfacial boundary condition for discontinuous electric field

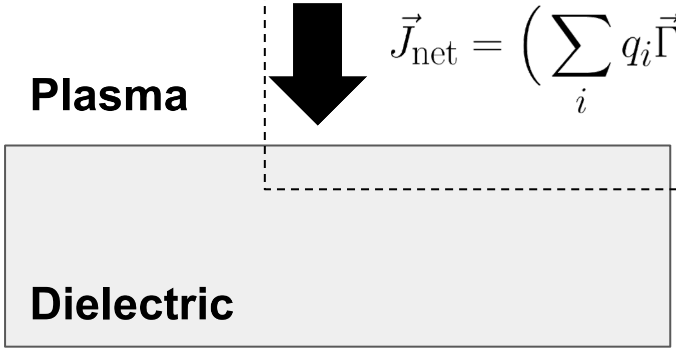

$$\vec{J}_{\text{net}} = \left(\sum_i q_i \vec{\Gamma}_i - q_e \vec{\Gamma}_e \right) \cdot \hat{n}$$

$$\frac{d\sigma}{dt} = \vec{J}_{\text{net}}$$

$$(\epsilon_p \nabla \phi_p - \epsilon_d \nabla \phi_d) \cdot \hat{n} = \sigma$$

2. Upgrades of Zapdos

2.3 Include heavy species solvation and evaporation boundary conditions

- A two-way interfacial transport model was added to Zapdos to allow neutral species to transport between gas and liquid phases based on Henry's law
  a. Henry coefficient, H, defines equilibrium concentration of species at interface
  b. Flux equality at the interface allows species to naturally flow in or out of the liquid

- While Henry's law is an equilibrium relationship, but only a ***local*** equilibrium at the interface is assumed - no assumption about bulk concentrations is made

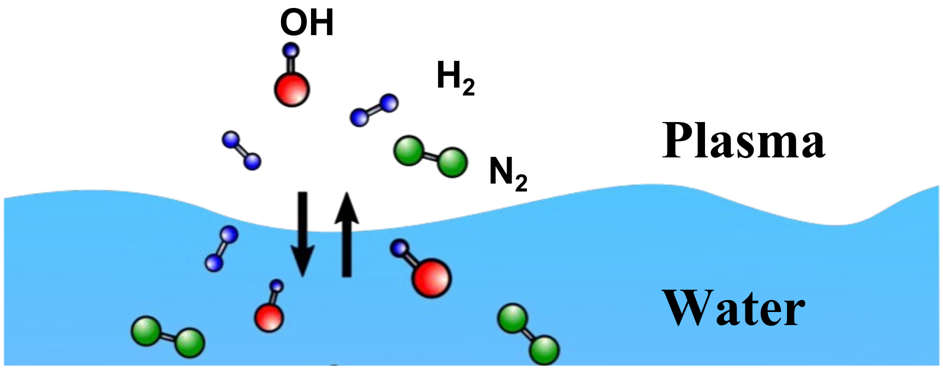

Henry's Law (local at the interface):

$$Hn_G = n_L$$

Flux Equality:

$$D_G \nabla n_G = D_L \nabla n_L$$

Verification and Validation of Zapdos-Crane (1/2)

- **Both codes were verified against multiple known problems; two examples:**

Crane vs. ZDPlasKin
(0D reaction networks)

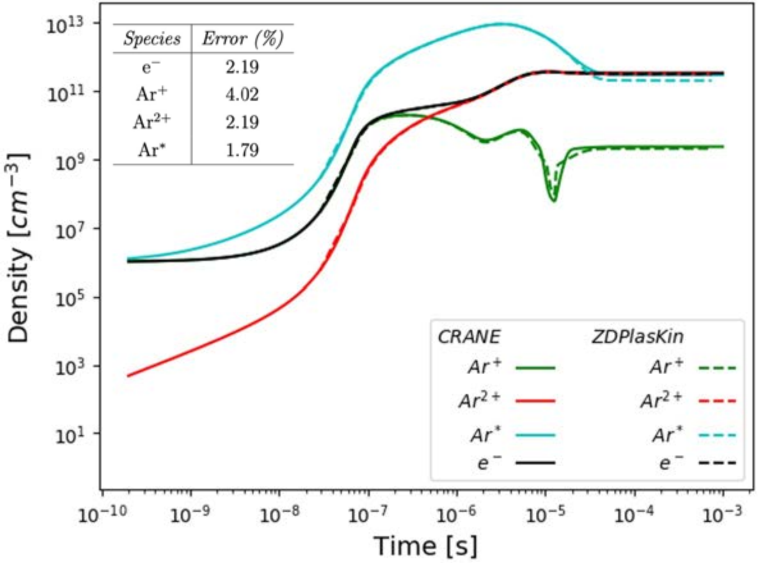

Zapdos-Crane vs. Comsol
(1D Dielectric Barrier Discharge)

Zapdos-Crane

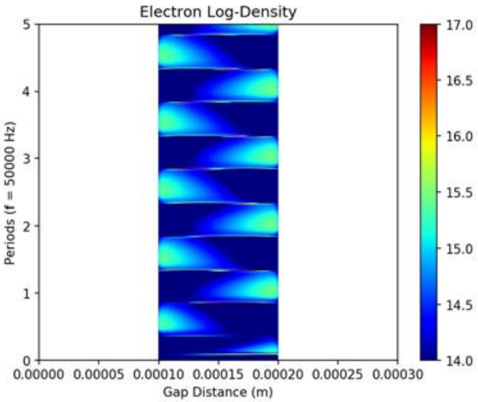

Comsol

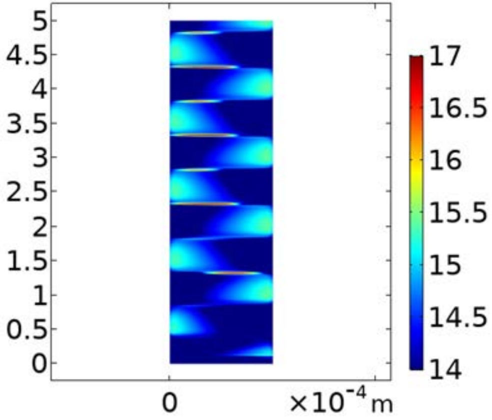

Verification and Validation of Zapdos-Crane (2/2)

- **Verification & Validation extended to:**
  - Multiple Analytical Solutions
  - Method of Manufactured Solutions (MMS)
  - 1D and 2D Capacitively Coupled Plasma and GEC Reference Cell

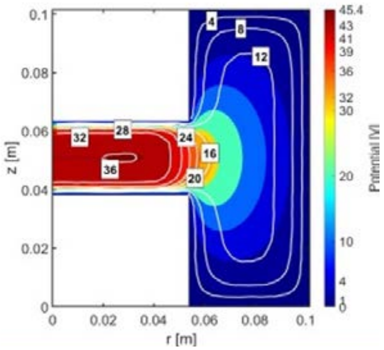

- **See ongoing work on V&V:**
  - C. DeChant, C. Icenhour, S. Keniley, A. Lindsay, G. Gall, K. Clein Hizon, D. Curreli, S. Shannon, Verification methods for drift–diffusion reaction models for plasma simulations, *Plasma Sources Science and Technology*, Volume 32, Number 4, (2023) https://doi.org/10.1088/1361-6595/acce65
  - C. DeChant, C. Icenhour, S. Keniley, G. Gall, A. Lindsay, D. Curreli, S. Shannon, Verification and validation of the open-source plasma fluid code: Zapdos, *Computer Physics Communications*, Volume 291, 108837 (2023) https://doi.org/10.1016/j.cpc.2023.108837

Typical Workflow

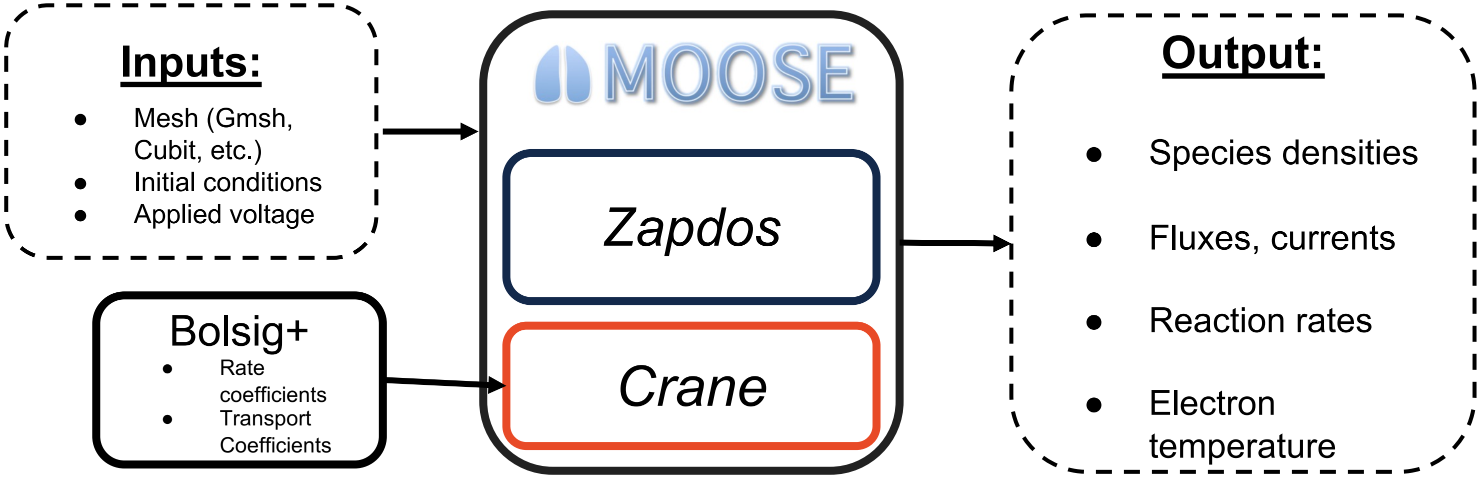

Zapdos-Crane was presented at a 2018 APS-GEC Workshop as an open-source plasma tool :

[8] C. Icenhour, S. Keniley, C. DeChant, C. Permann, A. Lindsay, R. Martineau, D. Curreli, S. Shannon, Multi-Physics Object Oriented Simulation Environment (MOOSE), Bull. Am. Phys. Soc. 71th Annual Gaseous Electronic Conference, BM2.1, Portland, Oregon, Nov 5-9, 2018

https://github.com/lcpp-org/crane

https://github.com/shannon-lab/zapdos

Model of the Plasma-Water Interface in Zapdos-Crane

- **Water region assumed to behave as a “dense plasma”:**
  - Same drift-diffusion-reaction equations apply
  - Higher background density
  - Relative permittivity of 81

Assumptions:

- **Electrons solvate instantly in water phase**
  - Solvation time estimated to be O(fs)
- **Heat transport is neglected (recently relaxed)**
- **Electron temperature is not considered in water**

Plasma Region:

$$\frac{\partial n_s}{\partial t} + \nabla \cdot \vec{\Gamma}_s = R_{sr}$$

$$-\nabla^2 \phi = \frac{(\sum_i q_i n_i + q_e n_e)}{\epsilon_0}$$

Water Region:

$$\frac{\partial n_{s,aq}}{\partial t} + \nabla \cdot \vec{\Gamma}_{s,aq} = R_{sr,aq}$$

$$-\nabla^2 \phi = \frac{(\sum_i q_i n_i + q_e n_e)}{\epsilon_0}$$

Electrons directly drift and diffuse into water:

$$\vec{\Gamma}_{e,\text{liquid}} \cdot \hat{n} = -\vec{\Gamma}_{e,\text{gas}} \cdot \hat{n}$$

Heavy Species Solvation (Henry’s Law):

$$H n_G = n_L$$

$$D_G \nabla n_G = D_L \nabla n_L$$

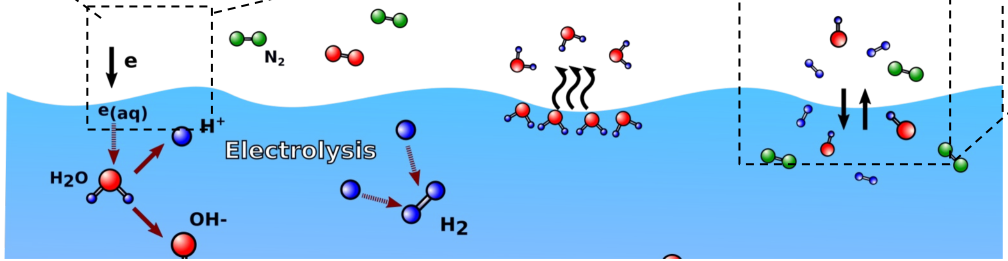

[10] Shane Keniley, Davide Curreli, Corey DeChant, and Steve Shannon, Numerical Modeling of the Plasma-Liquid Interface using the Zapdos-CRANE Open-Source Package, 72nd Annual Gaseous Electronics Conference, College Station, Texas, October 28-November 1, 2019

Case Study: Plasma Electrochemical Cell

- Argon plasma on liquid water
- Electrochemical cell
  - 66.6 mm-wide borosilicate cell
  - Gas-tight PFTE lid
  - Stainless steel needle electrode
  - DC discharge across 1 mm gap
- Liquid
  - Deionized water (HPLC grade)
  - NaCl 20 mM
- DC power supply
  - ±2500V applied voltage, changed to control the current
  - R_B = 651kΩ ballast resistor

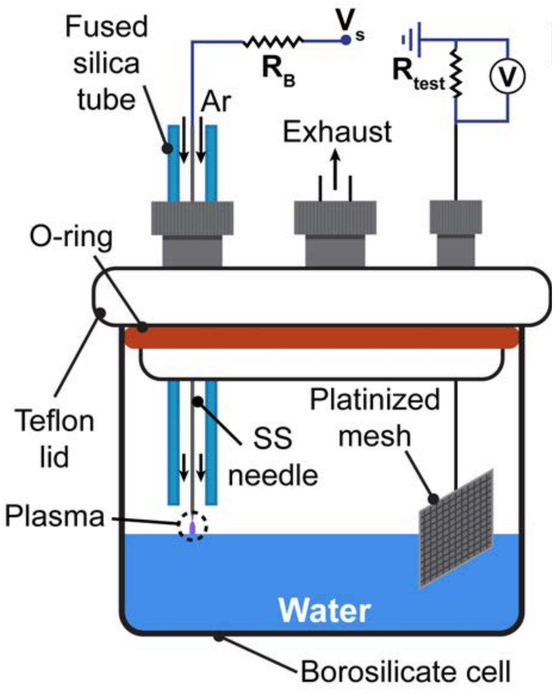

Schematic of the plasma electrochemical cell

Anodic vs. Cathodic operation

Anodic operation

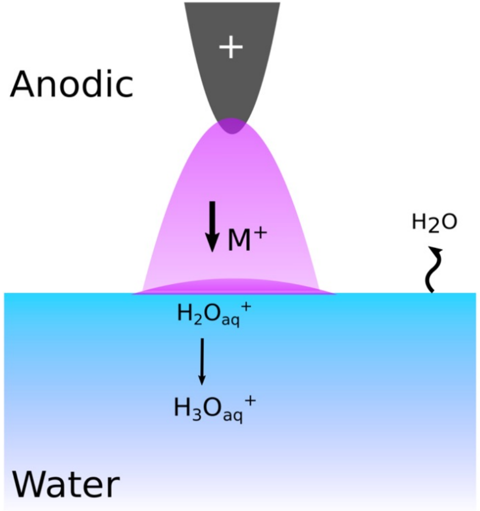

Cathodic operation

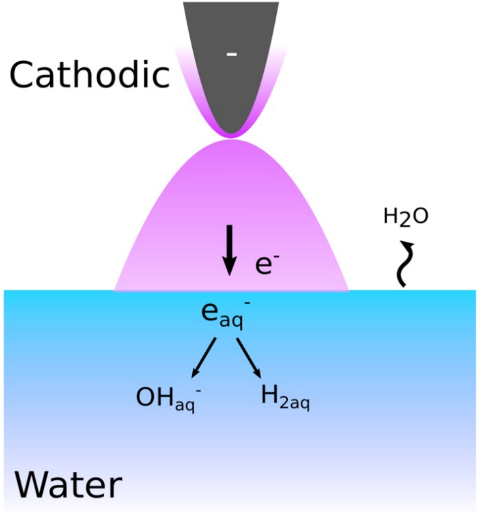

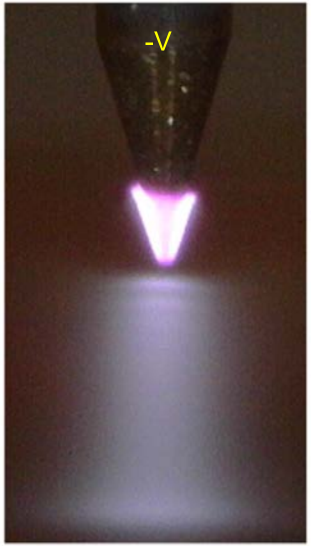

Charged and Neutral Species in the Gas/Liquid

	Charged Species	Neutrals
Plasma	e^- Ar^+ Ar_2^+ H_2O^+ OH^+ OH^-, O^-, O_2^-, O_2^+ H^+ O^+ H^-, H_3O^+ ArH^+	Ar^*, Ar^{**}, Ar^{***}, Ar_2^* H_2O, OH, O_2, O_2^*, O, O^*, H_2, H, H^*, O_3, HO_2, H_2O_2, OH^*, H_2Ov
Water	e_{aq}^- $H_3O_{aq}^+$ OH_{aq}^- $O2_{aq}^-$ O_{aq}^- HO_{2aq}^- $H_2O_{aq}^+$ O_{3aq}^-	H_{aq} H_2O_{2aq} OH_{aq} O_{2aq} O_{aq} H_{2aq} HO_{2aq} O_{3aq} HO_{3aq}

Reactions: 301 gas-phase and 72 liquid-phase reactions

Number	Reaction
(R1)	$e + Ar \to e + Ar$
(R2)	$e + Ar \to e + Ar^{*}$
(R3)	$e + Ar \to e + Ar^{*}$
(R4)	$e + Ar \to e + Ar^{**}$
(R5)	$e + Ar \to e + Ar^{***}$
(R6)	$e + Ar^{*} \to e + Ar^{**}$
(R7)	$e + Ar^{*} \to e + Ar^{***}$
(R8)	$e + Ar^{**} \to e + Ar^{***}$
(R9)	$e + Ar \to 2e + Ar^{+}$
(R10)	$e + Ar^{*} \to 2e + Ar^{+}$
(R11)	$e + Ar^{**} \to 2e + Ar^{+}$
(R12)	$e + H^{-} \to 2e + H$
(R13)	$e + H_2O \to e + H_2O$
(R14)	$e + H_2O \to H_2O_v + e$
(R15)	$e + H_2O \to OH + H^{-}$
(R16)	$e + H_2O \to e + OH^{*} + H$
(R17)	$e + H_2O \to 2e + H_2O^{+}$
(R18)	$e + H \to e + H^{*}$
(R19)	$e + H^{*} \to e + H$
(R20)	$e + O_2 \to e + O_2$
(R21)	$e + O_2 \to O_2^{*} + e$
(R22)	$e + O_2 \to 2e + O_2^{+}$
(R23)	$e + O_2 \to 2e + O + O^{+}$
(R24)	$e + O_2^{*} \to e + O_2$
(R25)	$e + O_2^{*} \to 2e + O_2^{+}$
(R26)	$e + O_2^{*} \to 2e + O^{+} + O$
(R27)	$e + O_2 \to O^{-} + O$
(R28)	$e + O_2^{*} \to O^{-} + O$
(R29)	$e + H_2O \to OH^{-} + H$
(R30)	$e + H \to 2e + H^{+}$
(R31)	$e + O_2^{+} \to 2O$
(R32)	$e + Ar^{+} \to Ar^{***}$
(R33)	$2e + Ar^{+} \to Ar^{***} + e$
(R34)	$e + Ar_2^{*} \to Ar_2^{+} + 2e$
(R35)	$e + Ar_2^{+} \to 2Ar + e$
(R36)	$e + Ar_2^{+} \to Ar^{***} + Ar$
(R37)	$Ar^{*} + Ar_2^{*} \to Ar^{+} + 2Ar + e$
(R38)	$2Ar^{*} \to Ar + Ar^{+} + e$
(R39)	$2Ar^{**} \to Ar + Ar^{+} + e$
(R40)	$2Ar^{***} \to Ar + Ar^{+} + e$
(R41)	$Ar^{*} + 2Ar \to Ar + Ar_2^{*}$
(R42)	$Ar^{**} + 2Ar \to Ar + Ar_2^{*}$
(R43)	$Ar^{***} + 2Ar \to Ar + Ar_2^{*}$
(R44)	$Ar^{+} + 2Ar \to Ar + Ar_2^{+}$
(R45)	$2Ar_2^{*} \to Ar_2^{+} + 2Ar + e$
(R46)	$Ar_2^{*} + Ar \to 2Ar + Ar$
(R47)	$Ar_2^{*} + Ar \to Ar^{*} + 2Ar$
(R48)	$Ar_2^{*} + Ar \to Ar^{**} + 2Ar$
(R49)	$H_2O_v + Ar \to H_2O + Ar$
(R50)	$H_2O_v + H_2O \to 2H_2O$
(R51)	$H_2O_v + O_2 \to H_2O + O_2$
(R52)	$e + H_2O^{+} \to O + H_2$
(R53)	$e + H_2O^{+} \to O + 2H$
(R54)	$e + H_2O^{+} \to OH + H$
(R55)	$e + H_2O_2 \to H_2O + O^{-}$
(R56)	$e + H_2O_2 \to OH + OH^{-}$
	Arg
(R57)	$Ar^{*} + O_2 \to Ar + 2O$
(R58)	$Ar^{*} + O_2^{*} \to Ar + 2O$
(R59)	$Ar^{**} + O_2 \to Ar + 2O$
(R60)	$Ar^{***} + O_2 \to Ar + 2O$
(R61)	$Ar^{***} + O_2^{*} \to Ar + 2O$
(R62)	$Ar^{+} + O \to Ar + O^{+}$
(R63)	$Ar^{+} + O_2 \to Ar + O_2^{+}$
(R64)	$Ar^{+} + O_2^{-} \to Ar + O_2$
(R65)	$Ar^{+} + O_2^{-} \to Ar + 2O$
(R66)	$Ar^{+} + O^{-} \to Ar + O$
(R67)	$Ar_2^{+} + O_2 \to 2Ar + 2O$
(R68)	$Ar_2^{+} + O_3 \to 2Ar + O_2 + O$
(R69)	$Ar_2^{+} + O^{-} \to 2Ar + O$
(R70)	$Ar_2^{+} + O_2 \to 2Ar + O_2^{+}$
(R71)	$Ar_2^{+} + O_2^{-} \to 2Ar + 2O$
(R72)	$Ar_2^{+} + O_2^{-} \to 2Ar + O_2$
(R73)	$Ar_2^{+} + O_3 \to 2Ar + O_2^{+} + O$
	Oxygen-heavy
(R74)	$2O + Ar \to O_2 + Ar$
(R75)	$2O + O_2 \to 2O_2$
(R76)	$2O + H_2 \to O_2 + H_2$
(R77)	$2O + H_2O \to O_2 + H_2O$
(R78)	$2O + Ar \to O_2^{*} + Ar$
(R79)	$O + O^{+} + Ar \to O_2^{+} + Ar$
(R80)	$O + O^{-} \to O_2 + e$
(R81)	$O + O_2 + Ar \to O_3 + Ar$
(R82)	$O + O_2 + H_2 \to O_3 + H_2$
(R83)	$O + O_2 + H_2O \to O_3 + H_2O$
(R84)	$O + O_2^{-} \to O_2 + O^{-}$
(R85)	$O + O_2^{-} \to O_3 + e$
(R86)	$O + O_3 \to 2O_2$
(R87)	$O^{*} + O_2 \to O_2^{*} + O$
(R88)	$O^{*} + O_3 \to O_2^{*} + O_2$
(R89)	$O^{*} + Ar \to Ar + O$
(R90)	$O^{+} + O_2 \to O + O_2^{+}$
(R91)	$O^{-} + O_2 \to O_2^{-} + O$
(R92)	$O^{-} + O_2^{*} \to O_3 + e$
(R93)	$O^{-} + O_2^{+} + Ar \to O + O_2 + Ar$
(R94)	$2O_2^{*} \to O_2^{*} + O_2$
(R95)	$O_2^{*} + O_2^{-} \to 2O_2 + e$
(R96)	$O_2^{*} + O_3 \to 2O_2 + O$
(R97)	$O_2^{*} + Ar \to O_2 + Ar$
(R98)	$O_2^{*} + H_2 \to O_2 + H_2$
(R99)	$O_2^{*} + H_2O \to O_2 + H_2O$
(R100)	$O_2^{*} + O_3 \to O_2 + O_3$
(R101)	$O_2^{+} + O_2^{-} \to O_2 + 2O$
(R102)	$O_2^{+} + O_2^{-} + Ar \to 2O_2 + Ar$
(R103)	$O_2^{-} + Ar \to O_2 + e + Ar$
(R104)	$O_3 + Ar \to O + O_2 + Ar$
(R105)	$O_3 + H_2 \to O + O_2 + H$
(R106)	$O_3 + H_2O \to O + O_2 + H_2O$
	Argon-humi
(R107)	$Ar^{*} + H_2 \to Ar + 2H$
(R108)	$Ar^{*} + OH \to Ar + O + H$
(R109)	$Ar^{*} + OH \to Ar + OH^{*}$
(R110)	$Ar^{*} + H_2O \to Ar + OH + H$
(R111)	$Ar^{**} + H_2 \to Ar + 2H$
(R112)	$Ar^{**} + OH \to Ar + O + H$
(R113)	$Ar^{**} + OH \to Ar + OH^{*}$
(R114)	$Ar^{**} + H_2O \to Ar + OH + H$
(R115)	$Ar^{**} + H_2 \to Ar + 2H$
(R116)	$Ar^{***} + H_2 \to Ar + 2H$
(R117)	$Ar^{***} + OH \to Ar + O + H$
(R118)	$Ar^{***} + H_2O \to Ar + OH + H$
(R119)	$Ar^{+} + H \to Ar + H^{+}$
(R120)	$Ar^{+} + H_2O \to Ar + H_2O^{+}$
(R121)	$Ar^{+} + OH^{-} \to Ar + OH$
(R122)	$Ar_2^{*} + H_2 \to 2Ar + 2H$
(R123)	$Ar_2^{*} + H_2O \to 2Ar + OH + H$
(R124)	$Ar_2^{+} + H \to 2Ar + H^{+}$
(R125)	$Ar_2^{+} + H_2O \to 2Ar + H_2O^{+}$
(R126)	$Ar_2^{+} + OH^{-} \to 2Ar + OH$
(R127)	$Ar_2^{+} + OH^{-} \to 2Ar + O + H$
	Humid air-heavy
(R128)	$H + O + Ar \to OH + Ar$
(R129)	$H + O + O_2 \to OH + O_2$
(R130)	$H + O + H_2 \to OH + H_2$
(R131)	$H + O + H_2O \to OH + H_2O$
(R132)	$H + O^{+} \to H^{+} + O$
(R133)	$H + O_2 + Ar \to HO_2 + Ar$
(R134)	$H + 2O_2 \to HO_2 + O_2$
(R135)	$H + O_2 + H_2O \to HO_2 + H_2O$
(R136)	$H + O_2 + H_2 \to HO_2 + H_2$
(R137)	$H + O_2^{*} \to OH + O$
(R138)	$H + O_2^{-} \to HO_2 + e$
(R139)	$H + O_3 \to OH + O_2$
(R140)	$H + O_3 \to HO_2 + O$
(R141)	$2H + Ar \to H_2 + Ar$
(R142)	$2H + H_2 \to H_2 + H_2$
(R143)	$2H + H_2O \to H_2 + H_2O$
(R144)	$H + OH + Ar \to H_2O + Ar$
(R145)	$H + OH + O_3 \to H_2O + O_3$
(R146)	$H + OH^{-} \to H_2O + e$
(R147)	$H + HO_2 \to H_2 + O_2$
(R148)	$H + HO_2 \to 2OH$
(R149)	$H + HO_2 \to H_2O + O$
(R150)	$H + HO_2 \to H_2O + O^{*}$
(R151)	$H + H_2O \to OH + 2H$
(R152)	$H + H_2O \to OH + H_2$
(R153)	$H + H_2O_2 \to HO_2 + H_2$
(R154)	$H + H_2O_2 \to H_2O + OH$
(R155)	$H^{*} + O_2 \to H + O_2$
(R156)	$H^{*} + O_3 \to H + O_3$
(R157)	$H^{*} + O \to H + O$
(R158)	$H^{*} + H_2O \to H + H_2O$
(R159)	$H^{*} + H_2 \to H + H_2$
(R160)	$H^{*} + Ar \to H + Ar$
(R161)	$H^{+} + O \to H + O^{+}$
(R162)	$H^{+} + O^{-} \to H + O$
(R163)	$H^{+} + O^{-} + Ar \to H + O + Ar$
(R164)	$H^{+} + O^{-} + Ar \to OH + Ar$
(R165)	$H^{+} + O_2 \to H + O_2^{+}$
(R166)	$H^{+} + O_2^{-} \to H + O_2$
(R167)	$H^{+} + OH \to H + OH^{+}$
(R168)	$H^{+} + OH^{-} \to OH + H$
(R169)	$H^{+} + OH^{-} \to 2H + O$
(R170)	$H^{+} + H_2O \to H + H_2O^{+}$
(R171)	$H_2 + O \to OH + H$
(R172)	$H_2 + O^{+} \to OH^{+} + H$
(R173)	$H_2 + O^{-} \to H_2O + e$
(R174)	$H_2 + O^{-} \to OH^{-} + H$
(R175)	$H_2 + O_2 \to H + HO_2$
(R176)	$H_2 + O_2 \to 2O + H_2$
(R177)	$H_2 + O_2 \to 2OH$
(R178)	$H_2 + O_2^{-} \to OH^{-} + OH$
(R179)	$H_2 + OH \to H_2O + H$
(R180)	$H_2 + OH^{+} \to H_2O^{+} + H$
(R181)	$H_2 + HO_2 \to H_2O_2 + H$
(R182)	$H_2 + H_2O \to OH + H_2 + H$
(R183)	$OH + O \to H + O_2$
(R184)	$OH + O^{*} \to H + O_2$
(R185)	$OH + O^{+} \to OH^{+} + O$
(R186)	$OH + O^{+} \to O_2^{+} + H$
(R187)	$OH + O_2^{-} \to OH^{-} + O_2$
(R188)	$OH + O_3 \to HO_2 + O_2$
(R189)	$2OH \to H_2O + O$
(R190)	$2OH + Ar \to H_2O_2 + Ar$
(R191)	$2OH + O_2 \to H_2O_2 + O_2$
(R192)	$2OH + H_2 \to H_2O_2 + H_2$
(R193)	$2OH + H_2O \to H_2O_2 + H_2O$
(R194)	$2OH + O_3 \to H_2O_2 + O_3$
(R195)	$OH + OH^{*} \to H_2O + O$
(R196)	$OH + OH^{+} \to H_2O^{+} + O$
(R197)	$OH + HO_2 \to H_2O + O_2$
(R198)	$OH + H_2O_2 \to H_2O + HO_2$
(R199)	$OH^{*} + H_2O_2 \to HO_2 + H_2O$
(R200)	$OH^{*} + Ar \to OH + Ar$
(R201)	$OH^{*} + H_2O \to OH + H_2O$
(R202)	$OH^{*} + H_2 \to OH + H_2$
(R203)	$OH^{+} + O \to O_2^{+} + H_2$
(R204)	$OH^{+} + O^{-} \to O + OH$
(R205)	$OH^{+} + O^{-} \to 2O + H$
(R206)	$OH^{+} + O^{-} + Ar \to OH + O + Ar$
(R207)	$OH^{+} + O^{-} + H_2 \to OH + O + H_2$
(R208)	$OH^{+} + O^{-} + Ar \to HO_2 + Ar$
(R209)	$OH^{+} + O^{-} + H_2 \to HO_2 + H_2$
(R210)	$OH^{+} + O_2 \to OH + O_2^{+}$
(R211)	$OH^{+} + OH^{-} + Ar \to H_2O_2 + Ar$
(R212)	$OH^{+} + OH^{-} + H_2O \to H_2O_2 + H_2O$
(R213)	$OH^{+} + OH^{-} + H_2 \to H_2O_2 + H_2$
(R214)	$OH^{+} + H_2O \to H_2O^{+} + OH$
(R215)	$OH^{-} + O \to HO_2 + e$
(R216)	$OH^{-} + O^{+} + Ar \to HO_2 + Ar$
(R217)	$OH^{-} + O_2^{+} \to OH + O_2$
(R218)	$OH^{-} + O_2^{+} + Ar \to OH + O_2 + Ar$
(R219)	$OH^{-} + O_3 \to O_2^{-} + HO_2$
(R220)	$OH^{-} + H_2O^{+} \to OH + H_2O$
(R221)	$OH^{-} + H_2O^{+} \to O + H + H_2O$
(R222)	$OH^{-} + H_2O^{+} \to 2OH + H$
(R223)	$OH^{-} + H_2O^{+} \to O + H + OH + H$
(R224)	$OH^{-} + H_2O^{+} + Ar \to OH + H_2O + Ar$
(R225)	$OH^{-} + H_2O^{+} + H_2O \to OH + 2H_2O$
(R226)	$OH^{-} + H_2O^{+} + H_2 \to OH + H_2O + H$
(R227)	$HO_2 + O \to OH + O_2$
(R228)	$HO_2 + O_2^{*} \to OH + O_2 + O$
(R229)	$2HO_2 \to H_2O_2 + O_2$
(R230)	$2HO_2 + Ar \to H_2O_2 + O_2 + Ar$
(R231)	$2HO_2 + H_2 \to H_2O_2 + O_2 + H_2$
(R232)	$2HO_2 + H_2O \to H_2O_2 + O_2 + H_2O$
(R233)	$HO_2 + H_2O \to H_2O_2 + OH$
(R234)	$HO_2 + H_2O_2 \to OH + H_2O + O_2$
(R235)	$H_2O + O \to 2OH$
(R236)	$H_2O + O^{*} \to H_2 + O_2$
(R237)	$H_2O + O^{+} \to H_2O^{+} + O$
(R238)	$H_2O + O^{-} \to H_2O_2 + e$
(R239)	$H_2O + O_2^{-} \to H_2O + O_2 + e$
(R240)	$H_2O^{+} + O \to OH + H + O$
(R241)	$H_2O^{+} + O^{-} + Ar \to H_2O + O + Ar$
(R242)	$H_2O^{+} + O^{-} + H_2O \to H_2O + O + H_2($
(R243)	$H_2O^{+} + O^{-} + H_2 \to H_2O + O + H_2$
(R244)	$H_2O^{+} + O^{-} + Ar \to H_2O_2 + Ar$
(R245)	$H_2O^{+} + O^{-} + H_2O \to H_2O_2 + H_2O$
(R246)	$H_2O^{+} + O^{-} + H_2 \to H_2O_2 + H_2$
(R247)	$H_2O^{+} + O_2 \to H_2O + O_2^{+}$
(R248)	$H_2O^{+} + O_2^{-} \to OH + H + O_2$
(R249)	$H_2O^{+} + O_2^{-} + Ar \to H_2O + O_2 + Ar$
(R250)	$H_2O_2 + O \to HO_2 + OH$
(R251)	$H_2O_2 + O \to H_2O + O_2$
(R252)	$H_2O_2 + O^{*} \to H_2O + O_2$
(R253)	$e + H_3O^{+} \to H_2O + H$
(R254)	$e + H_3O^{+} \to H_2 + OH$
(R255)	$e + H_3O^{+} \to 2H + OH$
(R256)	$H_2 + H_2O^{+} \to H_3O^{+} + H$
(R257)	$OH + H_2O^{+} \to H_3O^{+} + O$
(R258)	$OH^{*} + H_2O \to H_3O^{+} + O$
(R259)	$OH^{-} + H_3O^{+} \to OH + H_2O + H$
(R260)	$OH^{-} + H_3O^{+} \to O + H + H_2O + H$
(R261)	$H_2O + H_2O^{+} \to H_3O^{+} + OH$
(R262)	$H_3O^{+} + O^{-} \to H_2O + H + O$
(R263)	$H_3O^{+} + O_2^{-} \to H_2O + H + O_2$
(R264)	$H_3O^{+} + O_2^{-} \to H_2O + H + 2O$
(R265)	$H_2O + ArH^{+} \to H_3O^{+} + Ar$
(R266)	$Ar^{+} + H_2 \to ArH^{+} + H$
(R267)	$Ar^{+} + H_2O \to ArH^{+} + OH$
(R268)	$Ar_2^{+} + H_2O \to ArH^{+} + Ar + OH$
(R269)	$OH^{-} + ArH^{+} \to Ar + H + OH$
(R270)	$OH^{-} + ArH^{+} \to Ar + H + O + H$
(R271)	$H_2O + ArH^{+} \to H_3O^{+} + Ar$
(R272)	$ArH^{+} + O^{-} \to Ar + O + H$
(R273)	$ArH^{+} + O^{-} + Ar \to 2Ar + O + H$
(R274)	$ArH^{+} + O_2^{-} \to Ar + O_2 + H$
(R275)	$ArH^{+} + O_2^{-} \to Ar + 2O + H$
(R276)	$Ar_2^{+} + H^{-} \to 2Ar + H$
(R277)	$H + O_2^{-} \to H^{-} + O_2$
(R278)	$H^{+} + H^{-} \to 2H$
(R279)	$H^{+} + H^{-} + Ar \to 2H + Ar$
(R280)	$H^{-} + O \to OH + e$
(R281)	$H^{-} + O_2 \to HO_2 + e$
(R282)	$H^{-} + O_2^{+} + Ar \to H + O_2 + Ar$
(R283)	$H^{-} + O_2^{+} + Ar \to HO_2 + Ar$
(R284)	$H^{-} + H_2O \to OH^{-} + H_2$
(R285)	$H^{-} + H_2O^{+} \to H_2O + H$
(R286)	$H^{-} + H_2O^{+} \to 2H + OH$
(R287)	$H^{-} + H_2O^{+} + Ar \to H + H_2O + A$
(R288)	$H^{-} + H_3O^{+} \to H_2 + H_2O$
(R289)	$H^{-} + H_3O^{+} + Ar \to H_2 + H_2O +$
(R290)	$H^{-} + Ar \to H + e + Ar$
(R291)	$H^{-} + ArH^{+} \to H_2 + Ar$
(R292)	$H^{-} + ArH^{+} \to 2H + Ar$
(R293)	$H_2 + O_2^{-} \to H^{-} + HO_2$
(R294)	$H_2 + OH^{-} \to H_2O + H^{-}$
	Radi
(R295)	$Ar^{***} \to Ar^{*}$
(R296)	$Ar^{***} \to Ar^{**}$
(R297)	$Ar^{*} \to Ar$
(R298)	$Ar^{**} \to Ar$
(R299)	$Ar_2^{*} \to 2Ar$
(R300)	$O_2^{*} \to O_2$
(R301)	$OH^{*} \to OH$

No	Reaction
(R1)	$e_{(aq)} + H_2O_{(aq)} \to H_{(aq)} + OH^{-}_{(aq)}$
(R2)	$e_{(aq)} + H_2O^{+}_{(aq)} \to H_{(aq)} + OH_{(aq)}$
(R3)	$e_{(aq)} + OH_{(aq)} \to OH^{-}_{(aq)}$
(R4)	$e_{(aq)} + H_3O^{+}_{(aq)} \to H_{(aq)} + H_2O_{(aq)}$
(R5)	$e_{(aq)} + H_2O_{2(aq)} \to OH_{(aq)} + OH^{-}_{(aq)}$
(R6)	$e_{(aq)} + HO^{-}_{2(aq)} \to OH_{(aq)} + 2OH^{-}_{(aq)}$
(R7)	$e_{(aq)} + O_{2(aq)} \to O^{-}_{2(aq)}$
(R8)	$e_{(aq)} + O_{(aq)} \to O^{-}_{(aq)}$
(R9)	$H_{(aq)} + OH_{(aq)} \to H_2O_{(aq)}$
(R10)	$H_{(aq)} + OH^{-}_{(aq)} \to e_{(aq)} + H_2O_{(aq)}$
(R11)	$H_{(aq)} + H_2O_{2(aq)} \to OH_{(aq)} + H_2O_{(aq)}$
(R12)	$H_{(aq)} + O_{2(aq)} \to HO_{2(aq)}$
(R13)	$H_{(aq)} + HO_{2(aq)} \to H_2O_{2(aq)}$
(R14)	$O_{(aq)} + H_2O_{(aq)} \to 2OH_{(aq)}$
(R15)	$O_{(aq)} + O_{2(aq)} \to O_{3(aq)}$
(R16)	$2OH_{(aq)} \to H_2O_{2(aq)}$
(R17)	$OH_{(aq)} + O^{-}_{(aq)} \to HO^{-}_{2(aq)}$
(R18)	$OH_{(aq)} + OH^{-}_{(aq)} \to O^{-}_{(aq)} + H_2O_{(aq)}$
(R19)	$OH_{(aq)} + HO_{2(aq)} \to H_2O_{(aq)} + O_{2(aq)}$
(R20)	$OH_{(aq)} + O^{-}_{2(aq)} \to OH^{-}_{(aq)} + O_{2(aq)}$
(R21)	$O^{-}_{(aq)} + H_2O_{(aq)} \to OH^{-}_{(aq)} + OH_{(aq)}$
(R22)	$O^{-}_{(aq)} + H_2O_{2(aq)} \to O^{-}_{2(aq)} + H_2O_{(aq)}$
(R23)	$O^{-}_{(aq)} + HO^{-}_{2(aq)} \to O^{-}_{2(aq)} + OH^{-}_{(aq)}$
(R24)	$O^{-}_{(aq)} + O_{2(aq)} \to O^{-}_{3(aq)}$
(R25)	$O^{-}_{(aq)} + O^{-}_{2(aq)} \to OH^{-}_{(aq)} + OH^{-}_{(aq)} + O_{2(aq)}$
(R26)	$OH_{(aq)} + H_2O_{2(aq)} \to H_2O_{(aq)} + HO_{2(aq)}$
(R27)	$OH_{(aq)} + HO^{-}_{2(aq)} \to OH^{-}_{(aq)} + HO_{2(aq)}$
(R28)	$H_2O^{+}_{(aq)} + H_2O_{(aq)} \to H_3O^{+}_{(aq)} + OH_{(aq)}$
(R29)	$H_3O^{+}_{(aq)} + OH^{-}_{(aq)} \to H_{(aq)} + OH_{(aq)} + H_2O_{(aq)}$
(R30)	$HO_{2(aq)} + H_2O_{(aq)} \to H_3O^{+}_{(aq)} + O^{-}_{2(aq)}$
(R31)	$H_3O^{+}_{(aq)} + O^{-}_{2(aq)} \to HO_{2(aq)} + H_2O_{(aq)}$
(R32)	$2O_{(aq)} \to O_{2(aq)}$
(R33)	$e_{(aq)} + O^{-}_{2(aq)} \to HO^{-}_{2(aq)} + OH^{-}_{(aq)}$
(R34)	$e_{(aq)} + HO_{2(aq)} \to HO^{-}_{2(aq)}$
(R35)	$e_{(aq)} + O^{-}_{(aq)} \to OH^{-}_{(aq)} + OH^{-}_{(aq)}$
(R36)	$e_{(aq)} + O^{-}_{3(aq)} \to O_{2(aq)} + 2OH^{-}_{(aq)}$
(R37)	$e_{(aq)} + O_{3(aq)} \to O^{-}_{3(aq)}$
(R38)	$H_{(aq)} + O_{(aq)} \to OH_{(aq)}$
(R39)	$H_{(aq)} + HO^{-}_{2(aq)} \to OH_{(aq)} + OH^{-}_{(aq)}$
(R40)	$H_{(aq)} + O^{-}_{3(aq)} \to OH^{-}_{(aq)} + O_{2(aq)}$
(R41)	$H_{(aq)} + O^{-}_{2(aq)} \to HO^{-}_{2(aq)}$
(R42)	$H_{(aq)} + O_{3(aq)} \to HO_{3(aq)}$
(R43)	$OH_{(aq)} + O^{-}_{3(aq)} \to O^{-}_{2(aq)} + HO_{2(aq)}$
(R44)	$OH_{(aq)} + O_{3(aq)} \to HO_{2(aq)} + O_{2(aq)}$
(R45)	$HO_{2(aq)} + O^{-}_{2(aq)} \to HO^{-}_{2(aq)} + O_{2(aq)}$
(R46)	$2HO_{2(aq)} \to H_2O_{2(aq)} + O_{2(aq)}$
(R47)	$HO_{2(aq)} + O_{(aq)} \to O_{2(aq)} + OH_{(aq)}$
(R48)	$HO_{2(aq)} + H_2O_{2(aq)} \to OH_{(aq)} + O_{2(aq)} + H_2O_{(aq)}$
(R49)	$HO_{2(aq)} + HO^{-}_{2(aq)} \to OH_{(aq)} + OH^{-}_{(aq)} + O_{2(aq)}$
(R50)	$2O^{-}_{2(aq)} + H_2O_{(aq)} \to H_2O_{2(aq)} + O_{2(aq)} + 2OH^{-}_{(aq)}$
(R51)	$O^{-}_{(aq)} + O^{-}_{2(aq)} \to 2OH^{-}_{(aq)} + O_{2(aq)}$
(R52)	$O^{-}_{2(aq)} + H_2O_{2(aq)} \to OH_{(aq)} + O_{2(aq)} + OH^{-}_{(aq)}$
(R53)	$O^{-}_{2(aq)} + HO^{-}_{2(aq)} \to O^{-}_{(aq)} + O_{2(aq)} + OH^{-}_{(aq)}$
(R54)	$O^{-}_{2(aq)} + O_{3(aq)} \to 2OH_{(aq)} + 2O_{2(aq)}$
(R55)	$O^{-}_{2(aq)} + O_{3(aq)} \to O^{-}_{3(aq)} + O_{2(aq)}$
(R56)	$O^{-}_{(aq)} + O^{-}_{2(aq)} \to OH^{-}_{(aq)} + HO^{-}_{2(aq)}$
(R57)	$O^{-}_{2(aq)} + H_{(aq)} \to O^{-}_{(aq)} + OH_{(aq)}$
(R58)	$O_{(aq)} + OH^{-}_{(aq)} \to HO^{-}_{2(aq)}$
(R59)	$O_{(aq)} + H_2O_{2(aq)} \to OH_{(aq)} + HO_{2(aq)}$
(R60)	$O_{(aq)} + HO^{-}_{2(aq)} \to OH_{(aq)} + O^{-}_{2(aq)}$
(R61)	$O_{3(aq)} + H_2O_{2(aq)} \to OH_{(aq)} + HO_{2(aq)} + O_{2(aq)}$
(R62)	$O^{-}_{3(aq)} + H_2O_{(aq)} \to O_{2(aq)} + OH_{(aq)} + OH^{-}_{(aq)}$
(R63)	$HO_{3(aq)} \to O_{2(aq)} + OH_{(aq)}$
(R64)	$H_2O_{2(aq)} \to 2OH_{(aq)}$
(R65)	$HO^{-}_{2(aq)} \to O^{-}_{(aq)} + OH_{(aq)}$
(R66)	$2e_{(aq)} \to H_{2(aq)} + 2OH^{-}_{(aq)}$
(R67)	$e_{(aq)} + H_{(aq)} \to H_{2(aq)} + OH^{-}_{(aq)}$
(R68)	[illegible]
(R69)	[illegible]
(R70)	[illegible]
(R71)	[illegible]
(R72)	[illegible]

Flow structure and gas temperature

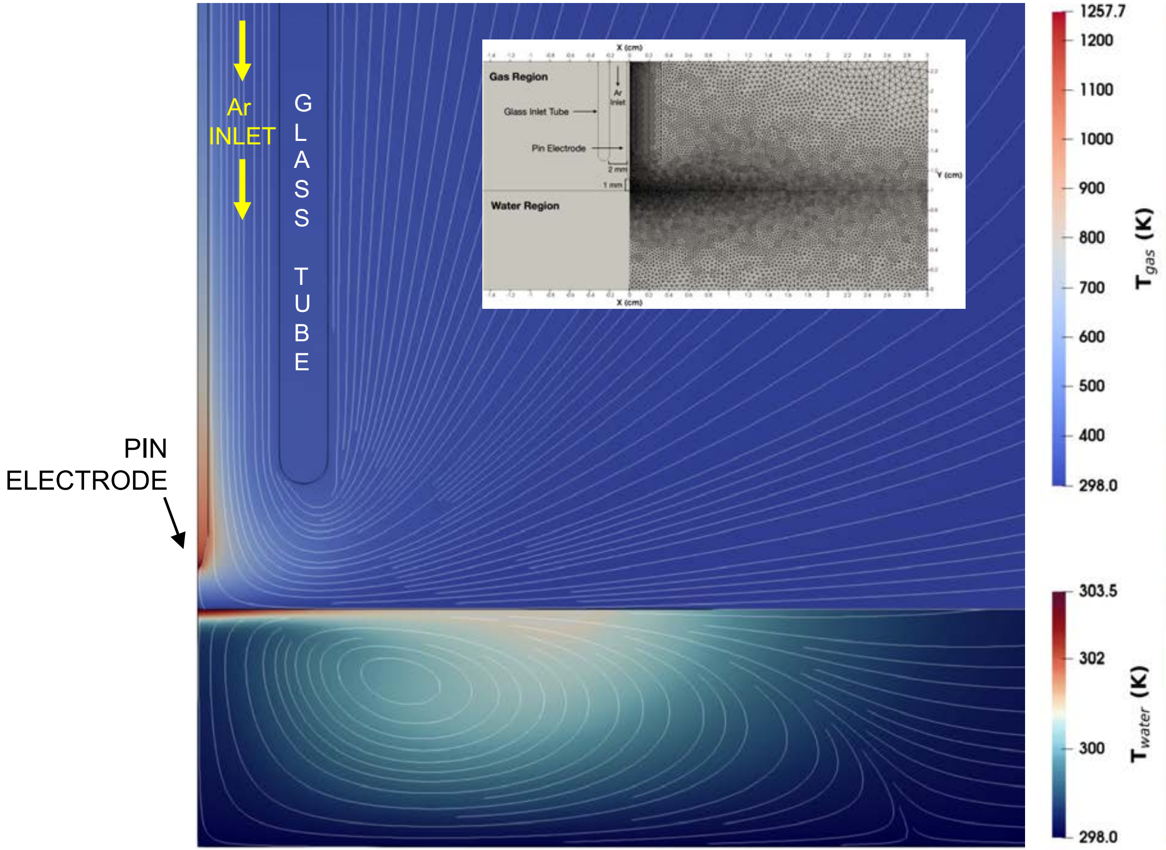

Ar/H_2O plasma on liquid water - Example of discharge evolution

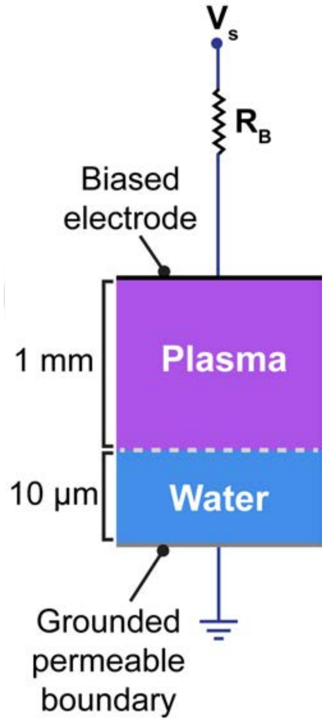

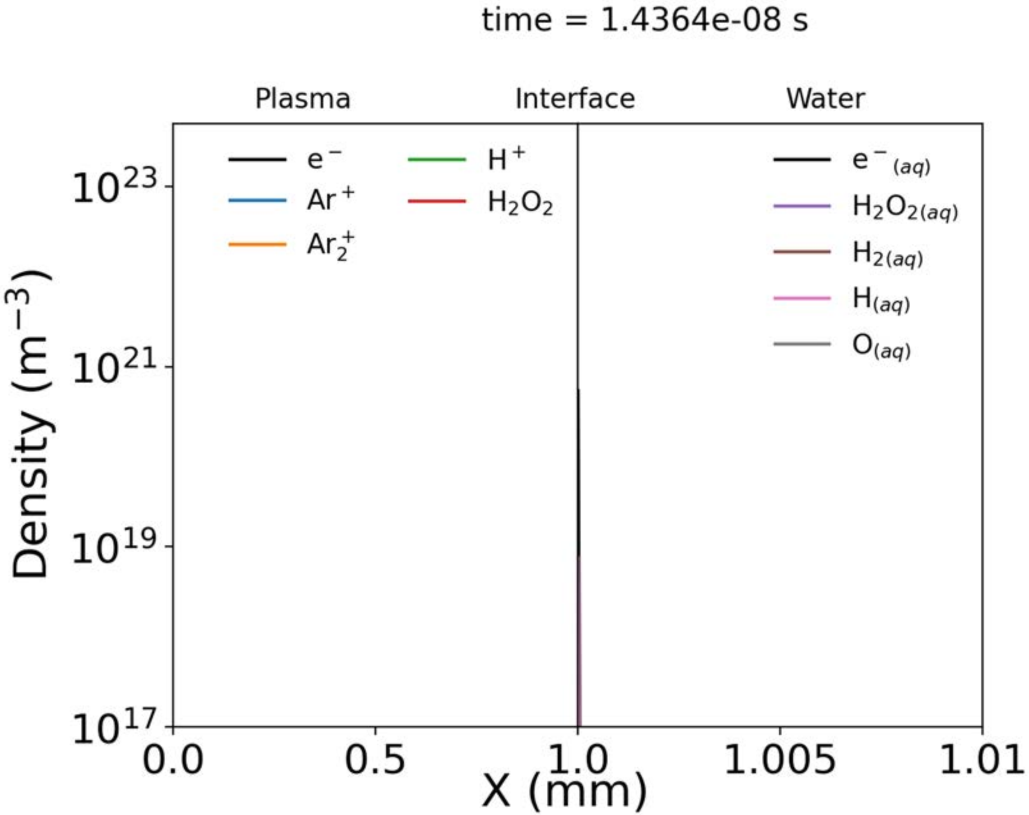

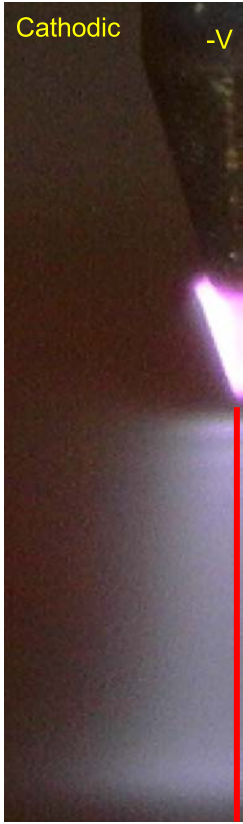

Electric Potential and Electric Field

Plasma Domain

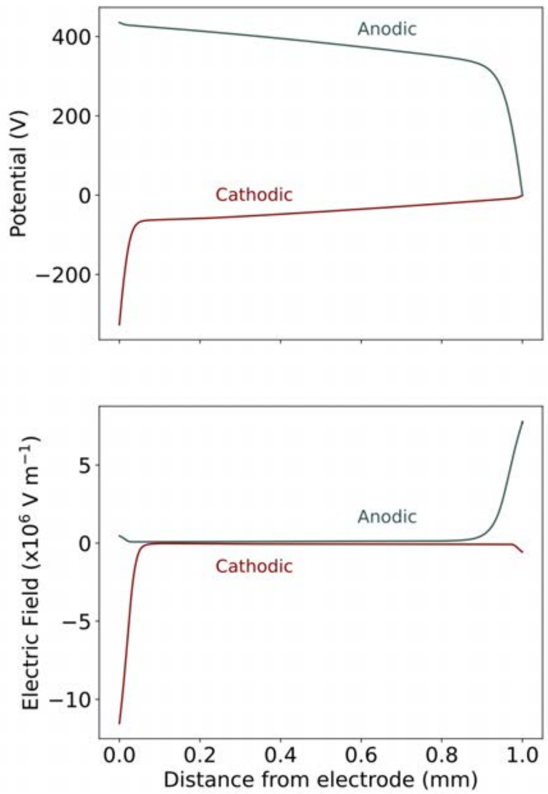

Water Domain

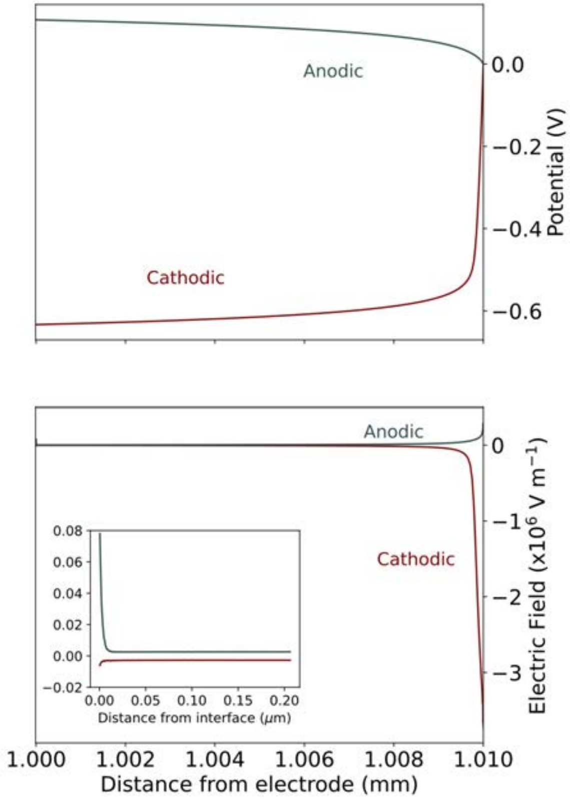

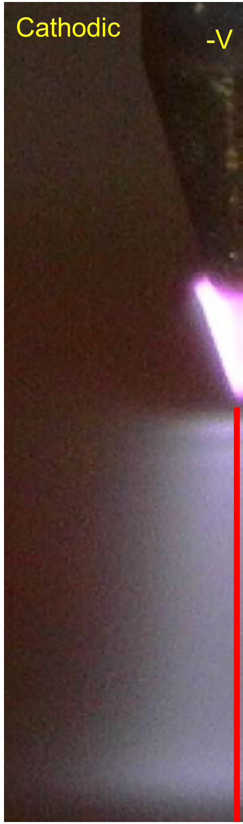

Electron Temperature at steady state, t > 100 ms

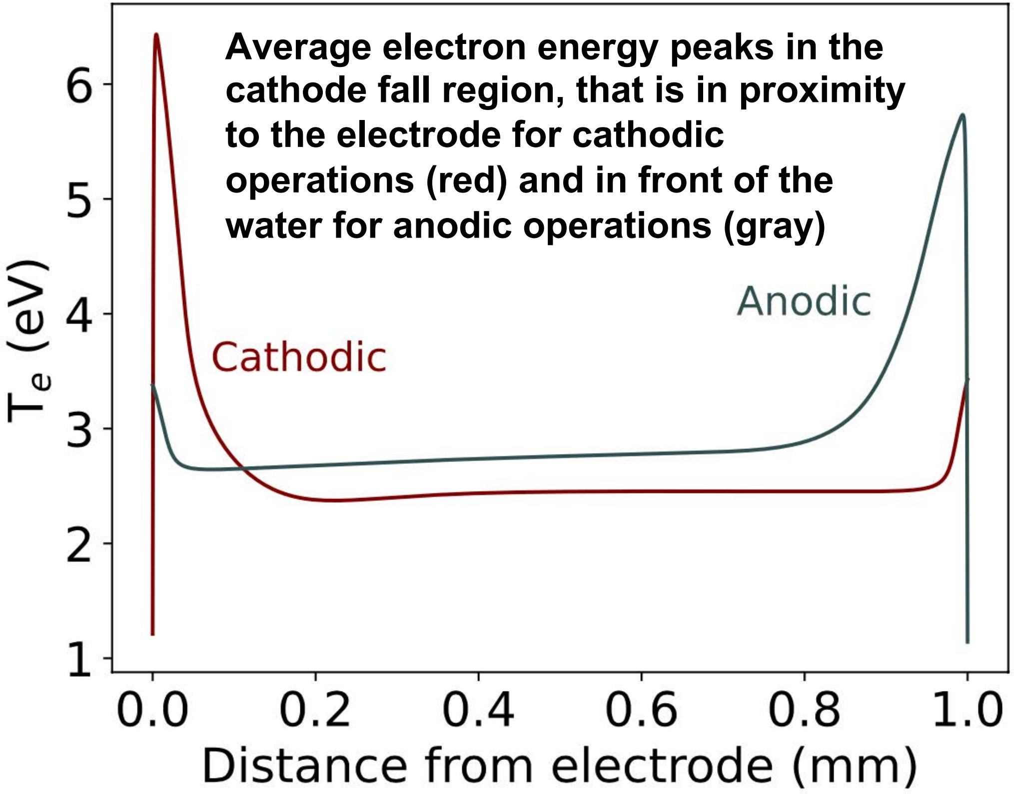

Density of selected species vs. time (volume averaged)

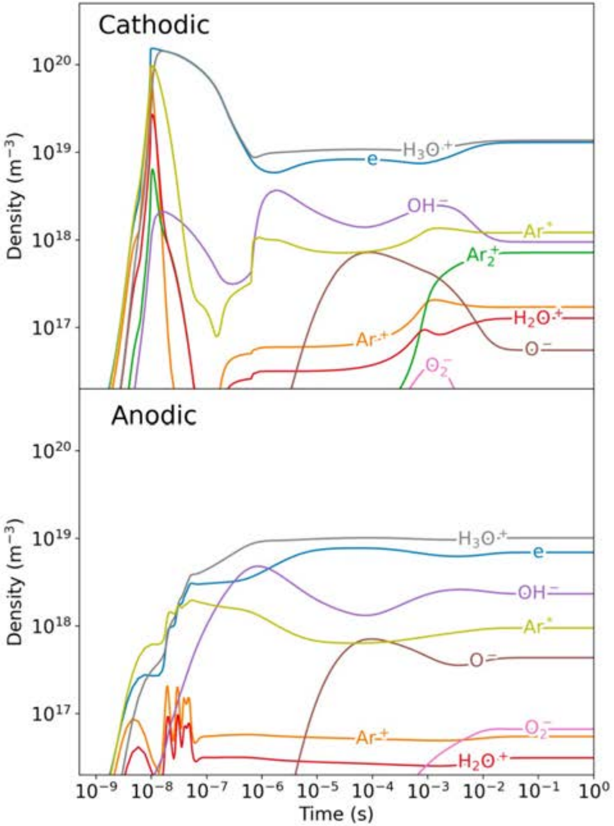

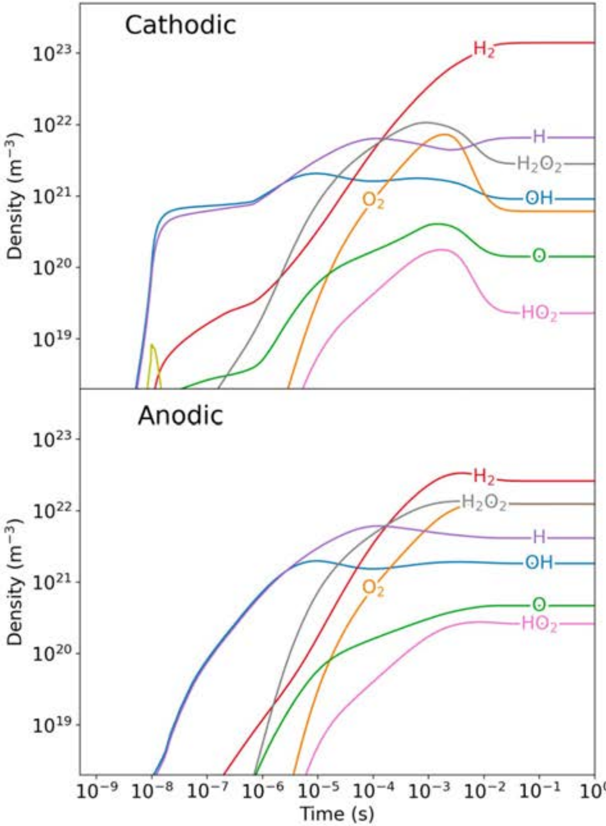

Density of selected species vs. position

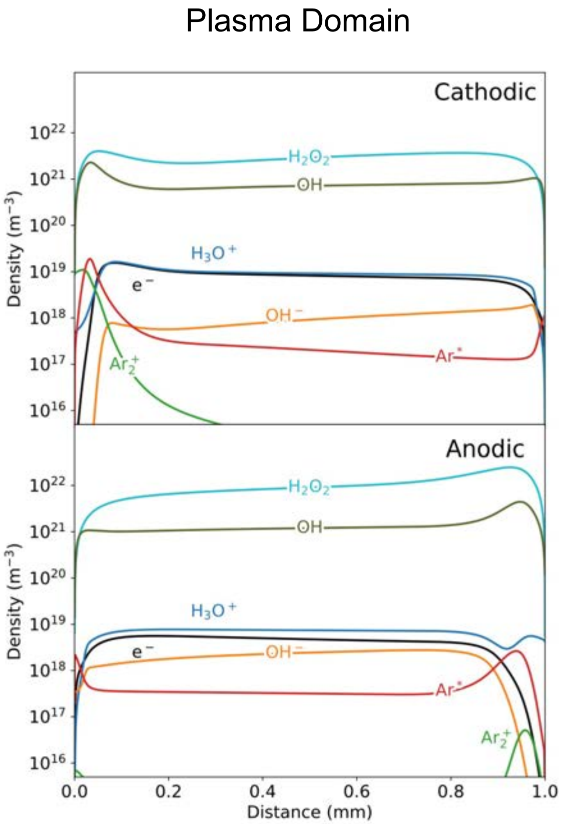

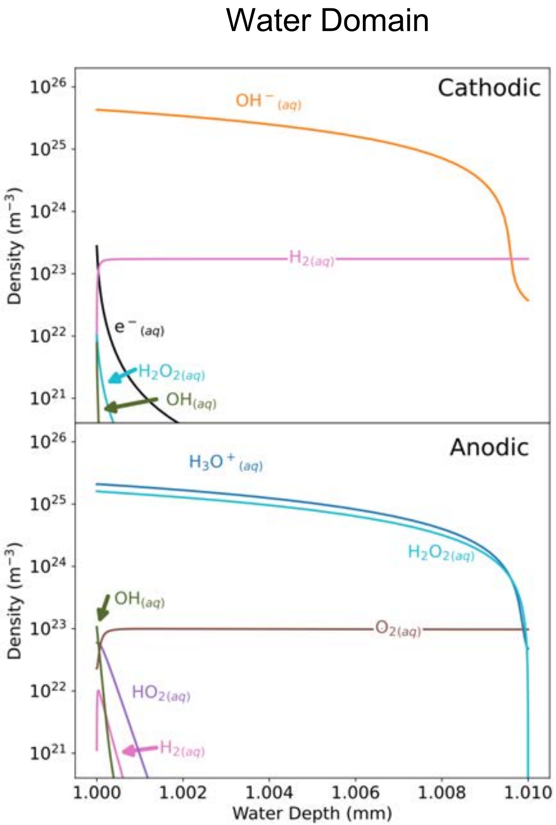

Reaction Mechanism in the Gas Phase during Cathodic Operations

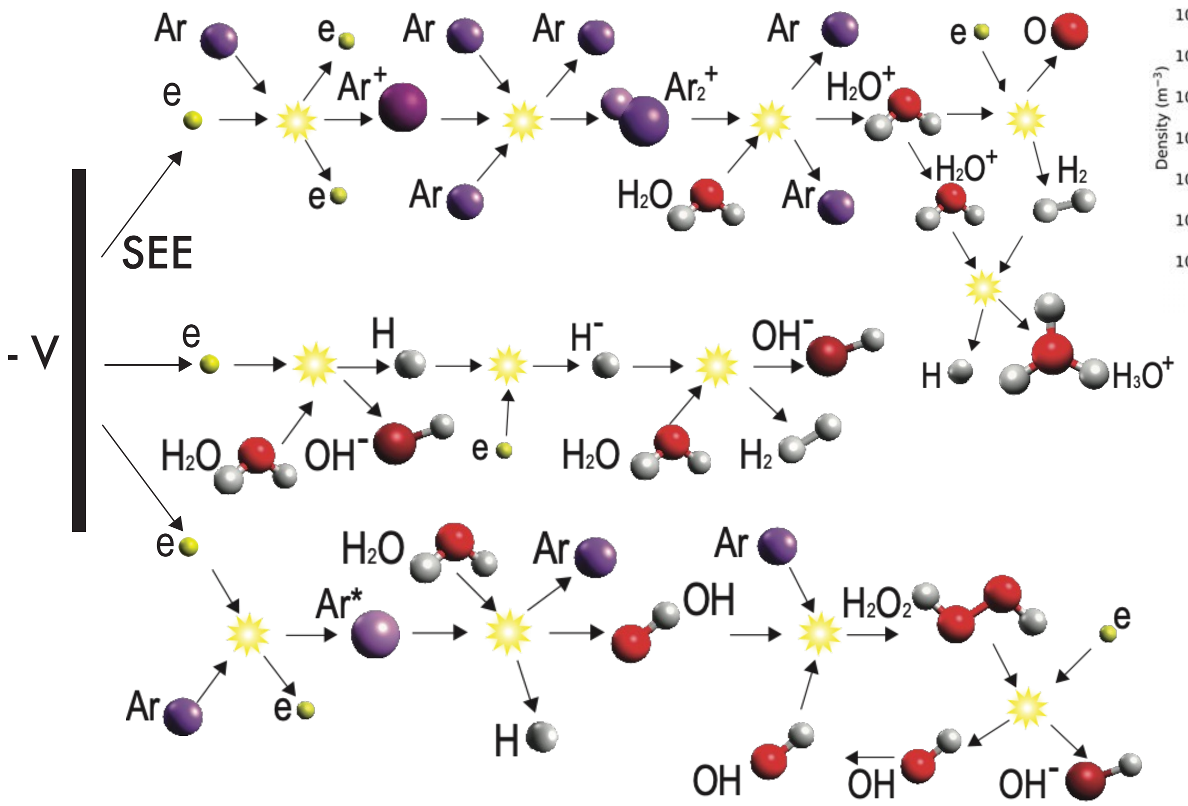

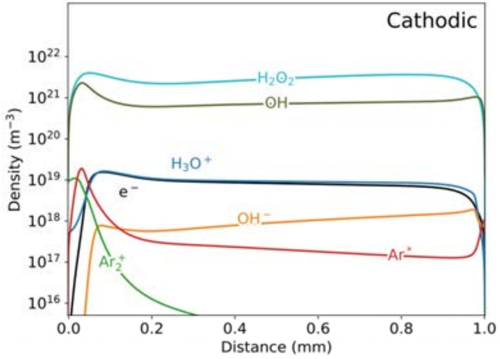

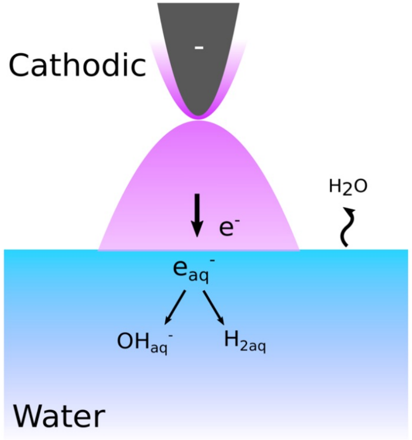

Reaction Mechanism during Anodic Operations

- Reaction mechanism is largely similar to the cathodic case, but with few fundamental differences
- Now positive species are accelerated toward the water
- Electrons move upward toward the positively-biased electrode
- Important: lack of solvated electrons in this case at the interface
- H_2, OH and H_2O_2 produced in the gas phase enter the water through dissolution
- In water, molecular oxygen is largely produced through the reaction

$$OH_{(aq)} + HO_{2(aq)} \rightarrow H_2O_{(aq)} + O_{2(aq)}$$

- O_2 production is in agreement with conventional electrolysis, where O_2 normally appears at the anode (+)

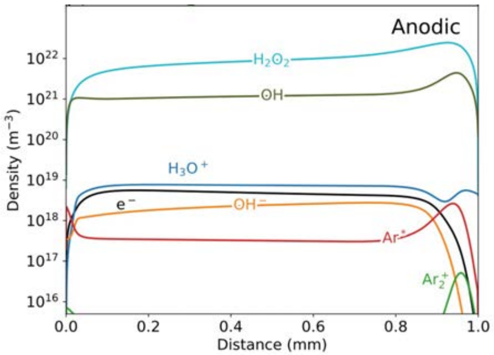

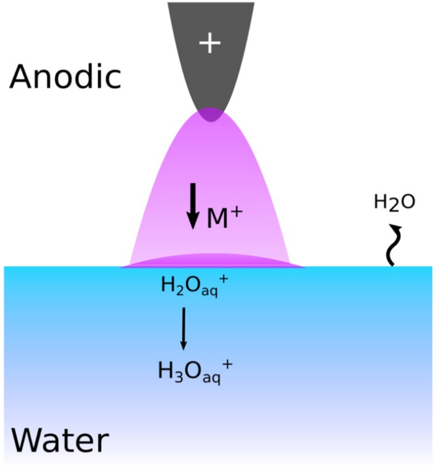

Hydrogen Peroxide – Generation Mechanism

- H_2O_2 is one of the predominant products
- Produced in the gas phase, mainly from OH
- Gaseous OH primarily forms in the cathode fall of the discharge through reactions with excited Ar states:

$$
\begin{aligned}
(Ar^*, Ar^{**}, Ar^{***}) + H_2O &\rightarrow Ar + OH + H \\
Ar_2^* + H_2O &\rightarrow 2Ar + OH + H \\
H + HO_2 &\rightarrow 2OH
\end{aligned}
$$

- Hydrogen peroxide is then formed through recombination of OH via three body reactions with neutral Ar and H_2O

$$
\begin{aligned}
2OH + Ar &\rightarrow H_2O_2 + Ar \\
2OH + H_2O &\rightarrow H_2O_2 + H_2O
\end{aligned}
$$

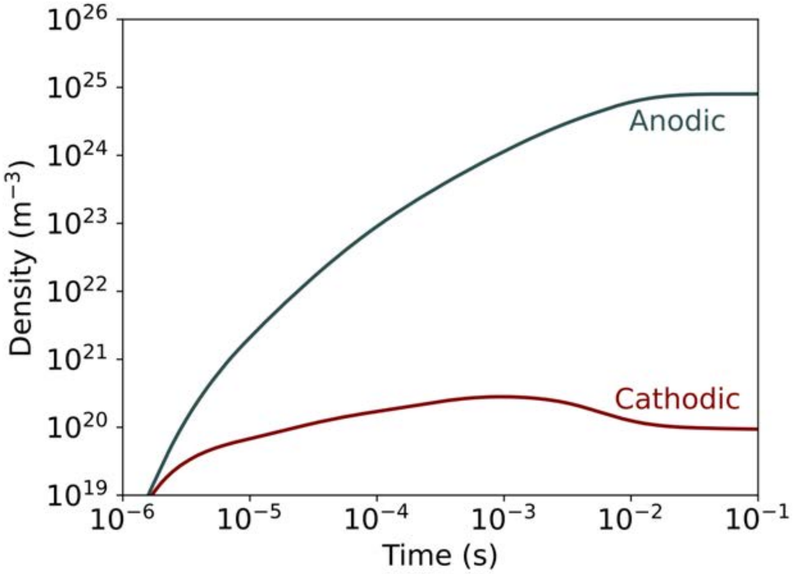

Average concentration of $H_2O_{2(aq)}$ over time in the 10 μm liquid film. In both cases $H_2O_{2(aq)}$ reaches steady state after ~10 ms, but in the anodic case the average value is over 4 orders of magnitude larger.

Hydrogen Peroxide – Generation Mechanism

- More H_2O_2 is produced in the anodic case for a number of reasons
- In the anodic case, T_e (average electron energy) is larger in front of the water surface
- Hence, density of excited Ar and ionized Ar is higher in front of the water surface
- Consequently, the production of OH and H_2O_2 peaks right in front of the water
- In addition, the concentration of solvated electrons in the first water layers is negligible in the anodic case with respect to the cathodic case!

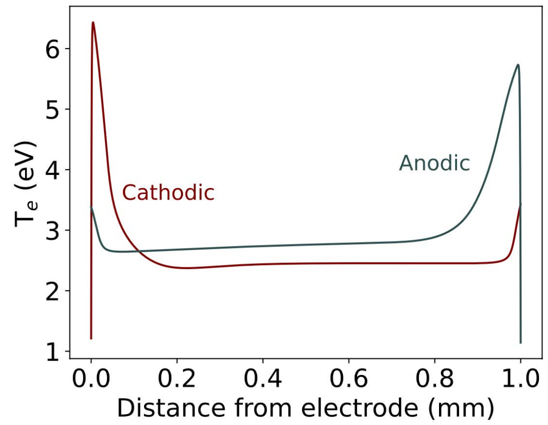

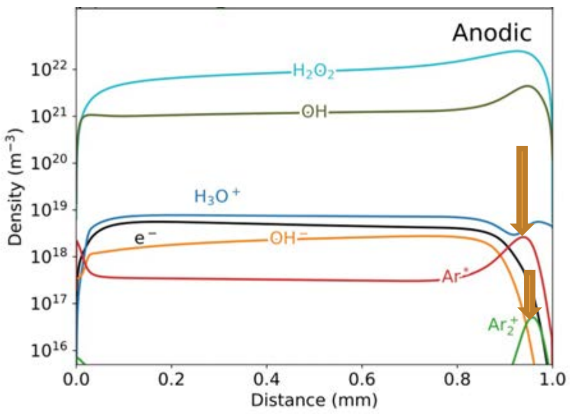

Solvated Electrons play a huge role in the consumption of $H_2O_{2(aq)}$

Dominant loss mechanisms for $H_2O_{2(aq)}$ in water

Anodic

Reaction	Percent (%)
$H_{(aq)} + H_2O_{2(aq)} \rightarrow OH_{(aq)} + H_2O_l$	62.15
$OH_{(aq)} + H_2O_{2(aq)} \rightarrow H_2O_l + HO_{2(aq)}$	35.86
$H_{2(aq)} + H_2O_{2(aq)} \rightarrow H_{(aq)} + OH_{(aq)} + H_2O_l$	1.34

Cathodic

Reaction	Percent
$e_{(aq)} + H_2O_{2(aq)} \rightarrow OH_{(aq)} + OH^-_{(aq)}$	99.09
$O^-_{(aq)} + H_2O_{2(aq)} \rightarrow O^-_{2(aq)} + H_2O_l$	0.47
$H_{(aq)} + H_2O_{2(aq)} \rightarrow OH_{(aq)} + H_2O_l$	0.34

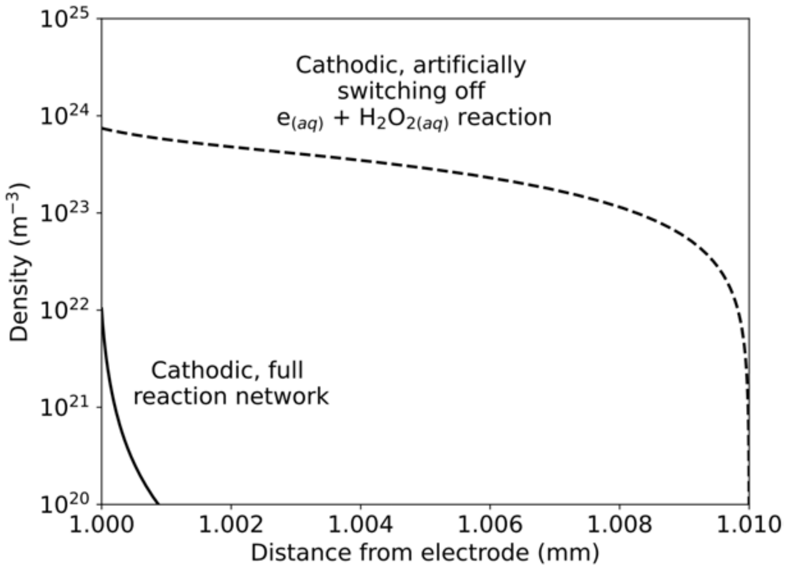

Aqueous hydrogen peroxide concentration at steady state in the cathodic case. The dotted line shows the concentration in the cathodic case with the reaction with solvated electrons switched off,
$e_{(aq)} + H_2O_{2(aq)} \rightarrow OH_{(aq)} + OH^-_{(aq)}$

Control experiment: NO_3^- electron scavenger in cathodic operations

- Control experiment was run in cathodic operations to understand the role of the "electron wall"
- Adding sodium nitrate ($NaNO_3$) to the solution
- Aqueous sodium nitrate fully dissociates into $Na^+_{(aq)}$ and $NO_3^-{}_{(aq)}$
- Resulting nitrate anions act as effective solvated electron scavengers, through the reduction

$$e_{(aq)} + NO^-_{3(aq)} \rightarrow NO^{2-}_{3(aq)}$$

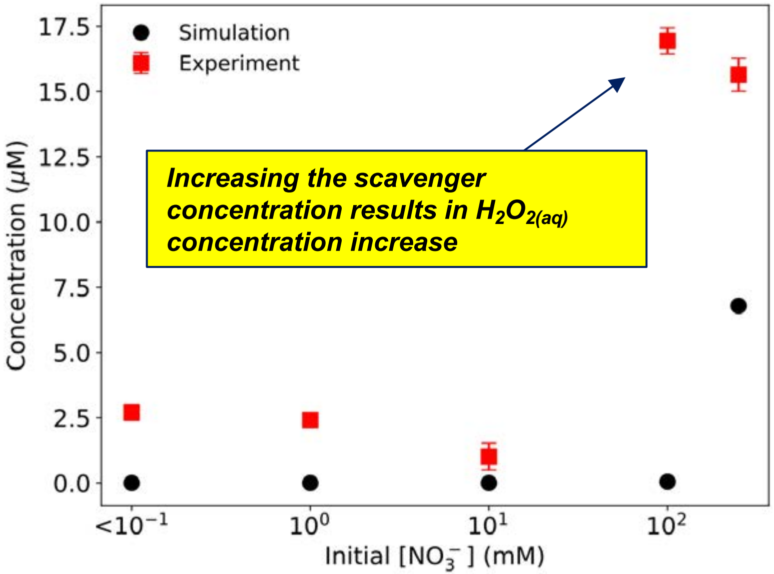

Experimental measurements of hydrogen peroxide concentration as a function of initial $NO_3^-{}_{(aq)}$ concentration added to the solution. Increasing the scavenger concentration from 10 to 100 mM results in $H_2O_{2(aq)}$ concentration increase from around 2.5 to 17 μM. Additional $NO_3^-{}_{(aq)}$ beyond 100 mM slightly decreases [$H_2O_{2(aq)}$].

Hydrogen Peroxide – Concentration, Model vs. Experiments

- $H_2O_{2(aq)}$ produced in plasma-liquid experiments was measured using two colorimetric assays:
    - titanium (IV) oxysulfate assay (TiOSO4)
    - ferrous oxidation-xylenol orange (FOX) assay
- $H_2O_{2(aq)}$ as a function of time at various discharge currents was compared to values predicted by the simulation
- Both simulations and measurements agree on the linear trend of increase of $H_2O_{2(aq)}$ concentration vs. time
- When scaled w.r.t the current, the simulation predicts a production rate 22% higher than the experiment

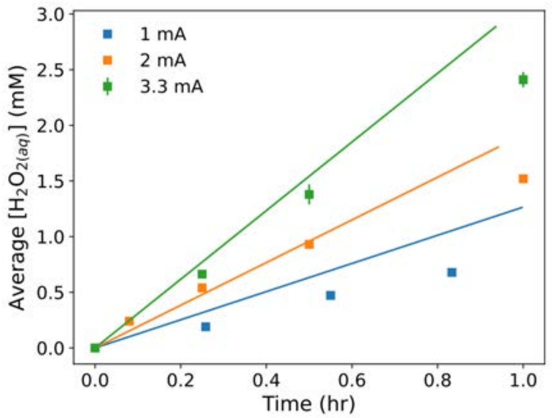

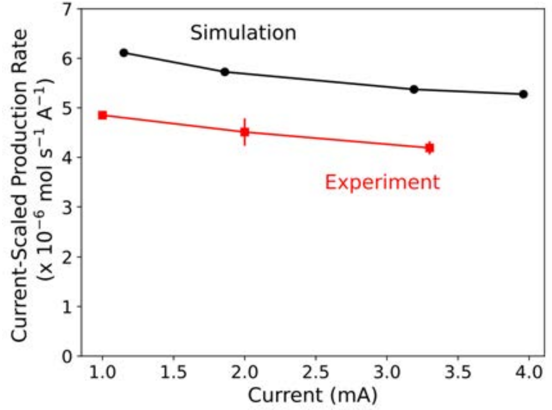

Solvated Electrons play a huge role in the consumption of $H_2O_{2(aq)}$

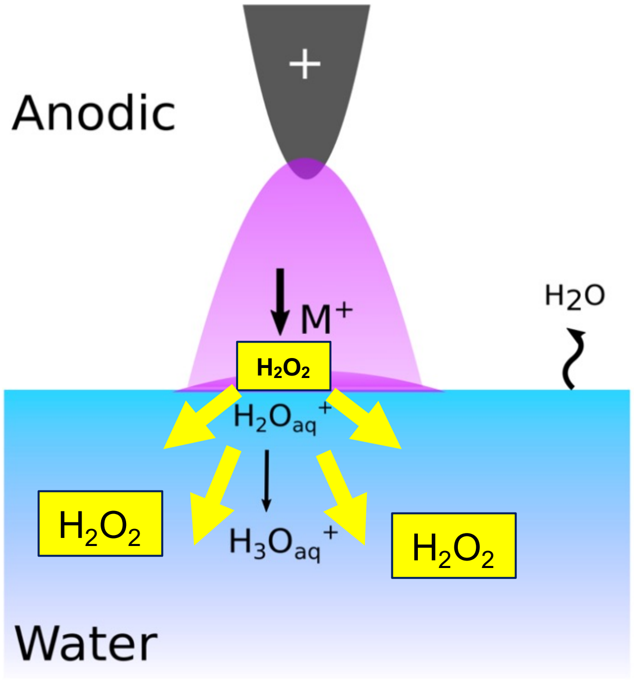

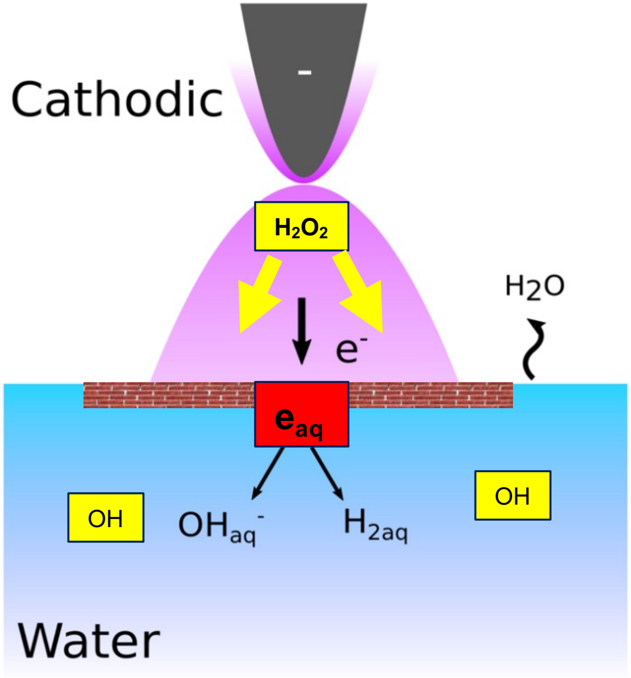

Conclusions

- Crane and Zapdos are two new, open-source, software applications based on the Moose framework, which can be used for the simulation of LTP with complex Plasma Chemistry
- We used the two new applications to study the problem of an argon plasma interfaced with liquid water, in both anodic and cathodic configuration
- We found that solvated electrons play a significant role in determining the production and destruction of chemical species and radicals in the system
- We looked at the production of hydrogen peroxide, finding that:
  - In **cathodic operations**, the layer of solvated electrons effectively dissociates H2O2, leaving only a negligible concentration inside the liquid.
  - In **anodic operations**, radicals are produced closer to the surface, and the layer of solvated electrons is almost not present; hydrogen peroxide can dissolve more easily into the liquid, where it remains present in significant concentrations useful for application purposes.
- To read more:
  - S. Keniley, Necip B. Uner, Elizabeth Perez, R. Mohan Sankaran, Davide Curreli, Multiphase Modeling of the Plasma-Water Interface: Application to Hydrogen Peroxide Generation with Experimental Validation, *Plasma Sources Science and Technology*, 31 (7), 075001 (2022) https://doi.org/10.1088/1361-6595/ac7891

Thanks!

LCPP Laboratory of Computational Plasma Physics – Codes

1. **Plasma Multi-Fluid Models**
   1. CRANE: Plasma Chemistry, https://github.com/lcpp-org/crane
   2. ZAPDOS: Plasma Transport, https://github.com/shannon-lab/zapdos
2. **Ion-Surface Interaction Models**
   1. RustBCA, https://github.com/lcpp-org/RustBCA
3. **Plasma Kinetic Models**
   1. hPIC (MPI/OpenMP) https://doi.org/10.1016/j.cpc.2018.03.028
   2. hPIC2 (+GPUs) https://doi.org/10.1016/j.cpc.2022.108569